Particle image velocimetry: A review

I Grant

Proceedings of the Institution of Mechanical Engineers, Part C: Journal of Mechanical Engineering Science 1997 211: 55
DOI: 10.1243/0954406971521665

Particle image velocimetry: a review

I Grant
Fluid Loading and Instrumentation Centre, Heriot-Watt University, Edinburgh, Scotland

Abstract: The evolution of particle image velocimetry (PIV) from its various roots is discussed. The importance of these roots and their influence on different trends in the speciality are described. The state-of-the-art of the technique today is overviewed and illustrated by reference to recent, seminal publications describing both the development and application of PIV.

Keywords: particle image velocimetry, fluid kinematics, multiple-exposure photographic methods

1 INTRODUCTION

1.1 The particle image velocimetry method

Particle image velocimetry (PIV) is a technique which allows the velocity of a fluid to be simultaneously measured throughout a region illuminated by a two-dimensional light sheet (see Fig. 1). 'Seeding' flow following particles are introduced into the flow and their motion used to estimate the kinematics of the local fluid. The particles are chosen to be near neutrally buoyant and to efficiently scatter light.

The motion of the particles is recorded using multiple-exposure photographic methods. From a knowledge of the time between recording the position of consecutive images together with the camera magnification the velocity of the particles is obtained. The recording parameters are chosen to obtain both good spatial separation of the images, ensuring accurate and reliable velocity measurements.

The MS was received on 10 October 1994 and was accepted for publication on 11 June 1996.

The illumination is most commonly provided by a laser, shaped into a planar 'sheet' using cylindrical lenses. An advantage of using a laser is that many lasers have a pulsed output with a pulse duration and a repetition rate making them suitable as a stroboscopic illumination source.

1.2 The development of photographic technology used in PIV

The development of photographic techniques, the mechanical shutter and the spark illumination system, in the mid-nineteenth century allowed the recording of high-speed motion. Examples include ballistic studies (Fig. 2a) and splashing liquids (Fig. 2b), one of the first examples of photographic flow visualization. An important method for recording three-dimensional images, photographic stereogrammetry, was developed in the late nineteenth century. These early developments have found new application in PIV, demonstrating that, as often in science, a new application leads to refreshed development and application.

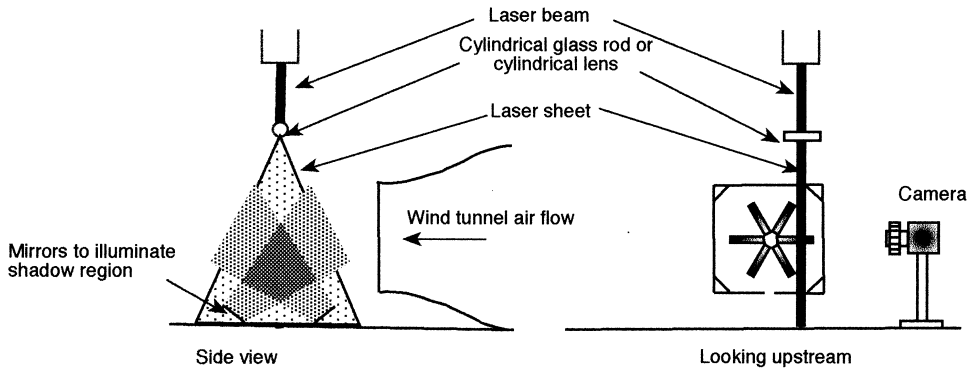

Fig. 1 Typical PIV experimental arrangement in use in a wind tunnel

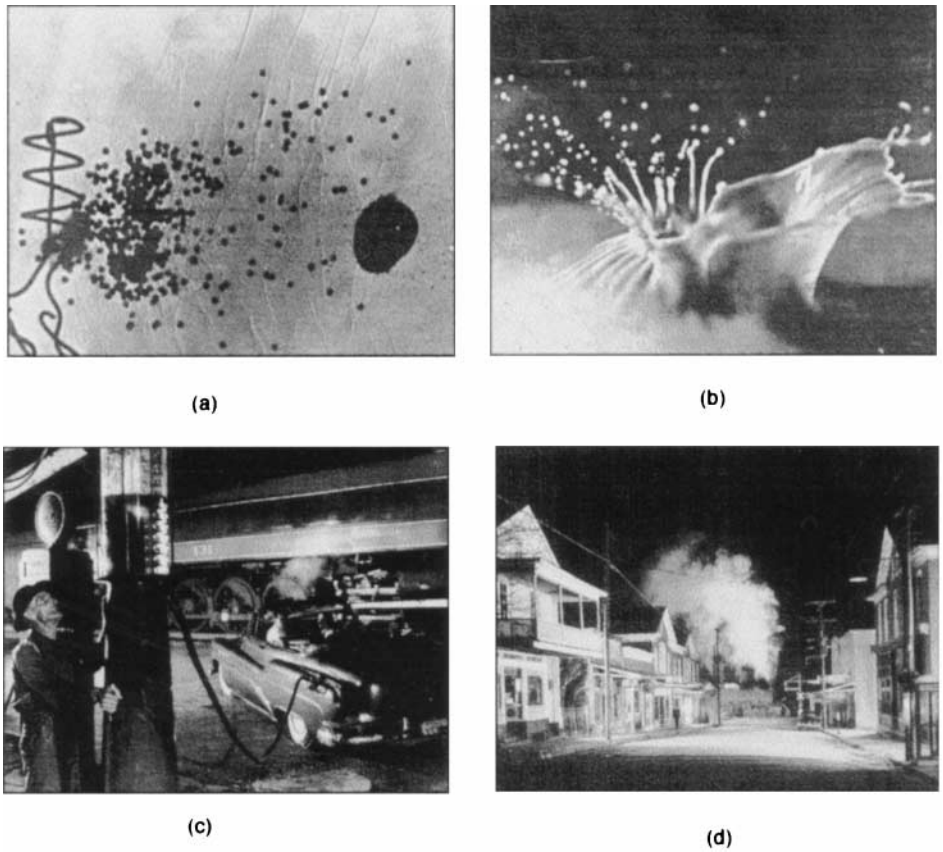

Fig. 2 Early examples of photographic motion arrestment. (a) Lead shot leaving a shotgun (Sir Charles de Boys, 1893). (b) Splashing liquid (Prof. E. M. Worthington, around 1900). (c) 'Sometimes the Electricity Fails, Vesuvius, Virginia' (O. Winston Link, 1956). (d) 'Ghost Town, Stanley, Virginia' (O. Winston Link, 1957). [(c) and (d) Copyright 1982 O. Winston Link, reproduced with his kind permission]

The important developments of the flash tube and stroboscope, by H. E. Edgerton, followed in the 1930s. One of the most evocative uses of this powerful flash photography can be seen in the work of O. Winston Link (Figs 2c and d) who, in the 1950s, made a definitive record of the final years of the steam locomotive in a series of stunning, synchronized pulsed illumination images. Winston Link's genius was to combine technology and art in stopping time both in a nostalgic and scientific sense. Many of his pictures provide visualizations of steam and smoke, seeding particles by another name, issuing from those wonderful machines inhabiting our yesterdays.

1.3 The evolution of particle image velocimetry

The rapid evolution of PIV was aided by parallel developments in optical measurement techniques, image processing, flow visualization and speckle metrology (**1**–**8**).

Speckle metrology is a method used for solid surface measurement (**9**). A diffuse laser beam falling on an optically rough surface leads to multiple light scattering, forming a 'speckle' interference pattern in the image plane of the observation optics. The characteristic highlights, or speckle, of the pattern are intimately related to the illuminated surface roughness and follow any movement.

The measurement of the motion of flows with a high concentration of seed particles was conceived as an extension of speckle metrology (**6**, **10**). In order to quantify the seeding density a resolution cell is defined in the fluid with a diameter equal to the projection of the particle image back into the flow. The cell height is taken as the light sheet thickness. The average number of particles found in the resolution cell is defined as the source density (**3**), N_s, where $N_s = \rho\, \Delta z\, \pi[d_I/(2M)]^2$, where ρ is the number of particles per unit volume (Fig. 3a). If $N_s \gg 1$, many particles occupy the resolution cell. Interference of the light scattered from these particles will occur in the image plane of the camera, forming a speckle pattern. The motion of the speckle pattern in the image plane is determined by the motion of the seeding particles in the flow. In principle the flow velocity can then be determined. In many flows this approach is limited in its application since the seeding density needed

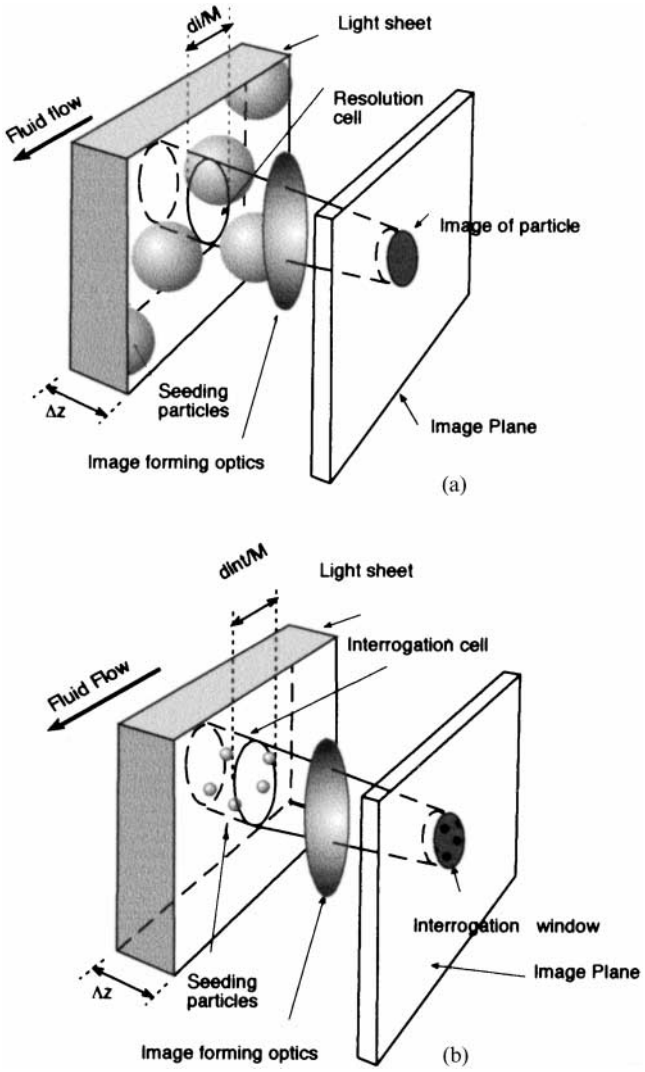

Fig. 3 Defining (a) source density and (b) image density

to produce speckle is impractical with such bulk loading potentially causing significant changes in the flow behaviour (**11**). The speckle pattern is also very sensitive to out-of (light)-plane motion (**12**), with the multiple exposures quickly becoming uncorrelated. Such out-of-plane motion is common in flows of practical importance where high levels of turbulence make the speckle velocimetry method unsuitable.

When the source density is low, $N_s \ll 1$, the flow measurement method is referred to as particle image velocimetry. This potentially powerful approach to flow measurement was first recognized as a separate method in the early 1980s (**13**, **14**). These first 'PIV' studies obtained photographic images containing a large number of particle images. In order to quantify the image density an interrogation cell is defined (**3**) as the intersection of the light sheet with the cylinder whose base has the area of the image interrogation window projected back into the fluid and whose height is that of the light sheet. The image density, N_I, is defined as the average number of particle images in the interrogation cell, $N_I = \rho\, \Delta z\, \pi[d_{int}/(2M)]^2$ (Fig. 3b). High image density corresponds to $N_I \gg 1$ while $N_I \ll 1$ corresponds to low image density.

1.4 Image capture

A number of important photographic parameters need to be considered when estimating the dynamic range of a flow measuring system based on the PIV method. These are discussed below.

1. *The spatial resolution* of an image capture system is determined by the vertex angle (α) of the cone of light (determined by the camera aperture $f^{\#}$) and the illuminating light wavelength λ. Ignoring constant multiplicative factors, the transverse resolution is given by the Rayleigh criterion as $d_1 \cong \lambda/\alpha$ and the longitudinal resolution as $d_2 \cong \lambda/\alpha^2$. For instance, at unit magnification, an $f^{\#}$ 2.8 lens gives a 6λ transverse resolution and a 30λ longitudinal resolution (**15**).
2. *Depth of field*. In order to obtain a sharp image the object particle needs to fall within the depth of field of the camera lens. This is the region in which the image is 'acceptably' sharp. The limits on image sharpness can be related to the diameter of the circle of confusion, the diameter of the disc in the image plane representing a point in the object plane. The depth of field (DOF) may be written as $2F(1 + 1/M)^2 f^{\#2}/10^6 M$ to a good approximation (**16**). Alternatively, DOF $= 4(1 + 1/M)^2 f^{\#2}\lambda$ (**17**). In principle, the use of a narrow-width laser sheet coincident with the in-focus plane may be used to ensure in-focus images. For example, if the particles are small and high spatial resolution is required $f^{\#} = 8$ and $\lambda = 0.6993$ μm may be taken, giving a depth of field of 0.7 mm. If a larger depth of field is required then the $f^{\#}$ must be increased with a resulting loss in resolution.
3. *Image size*. If the particle image can be resolved, its size will depend on the particle diameter, d_P, the lens magnification, M, and the point response function (PRF) of the lens. If the particle falls within the depth of field of the lens the geometrical image diameter is given by $d_{GI} = Md_P$. When the lens is diffraction limited the PRF is an Airy function of diameter $d_A = 2.44\ (1 + M)f^{\#}$. The image is obtained by convoluting the PRF with the geometrical image of the particle. An estimate of this effect can be obtained by replacing both the Airy function and the particle image by Gaussian functions, leading to the approximation for the image diameter $d_I = M^2 d_{GI}^2 + d_A^2$ (**18**).

   Typically, in a PIV experiment $M = 1$, $f^{\#} = 8$ and $\lambda = 0.6993$ μm. In this case $d_A = 25$ μm so d_I is effectively independent of particle size for particles less

than 10 μm in diameter. When $d_P > 50$ μm then the image size is effectively the geometrical particle image size.

4. *Recording medium*. The recording medium chosen is dependent on the size of flow field to be recorded and the required resolution. For example, a CCD (charge coupled device) (digital) camera of 512×512 pixels (digital picture elements) represents the image by 2.6×10^5 pixels whereas a large format photographic transparency (100 mm × 125 mm) of 300 lines/mm of film contains the equivalent of 1.1×10^9 pixels. Higher resolution CCD cameras are now available using a 2048×2048 format (or higher in specialist cameras). This means that single-image files may contain 42×10^5 pixels. This has implications for speed in the data handling and storage by the host computer. The CCD camera captures data at the video framing rate of 25 frames/s, with the digital image data being passed to a frame board storage, on-board processing and forwarding to digital memory.

1.5 Particle dynamics

The effectiveness of the particles in following the flow can be determined from a knowledge of particle dynamics in two-phase flow conditions. The possibility that the local flow conditions might concentrate (**19**) or disperse (**20**) the particles needs also to be considered since this could lead to velocity bias errors.

Most treatments of the behaviour of seeding particles use the argument of Stokes for low Reynolds's number flow around a sphere as a starting point. Particle inertial force terms are neglected and the drag force taken as $D = 3\pi\mu d_P U$, where μ is the viscosity, d_P is the diameter of the sphere and U is the relative velocity between the sphere and the fluid.

A small particle moving in a fluid is described by the equation of motion

$$\frac{\pi d_P^3}{6}\rho_P \dot{v} = 0.5 C_D \frac{\pi d_P^2}{4}\rho_F U^2$$

$$\Rightarrow U = \frac{d_P^2 \rho_P \dot{v}}{18\mu}$$

where ρ_P is the particle density and $\dot{v}$ is the particle acceleration. In the presence of spatial or temporal gradients in the fluid the ability of the particles to follow the gradients may be estimated from this equation. As the flow accelerates the inertia of the particles causes a delay in their response. Comparing the slip velocity with the fluid velocity gives an estimate of the measurement error. The particles have a characteristic response time and assume the velocity of the local flow exponentially (**1**, **21**).

Using this simple model of particle motion can lead to systematic errors in the resulting estimate fluid velocity in certain cases. Examples include the Saffman lift force experienced by a particle in shear flow (**22**) and the presence of significant centripetal forces in swirling flow. Assuming Stokes drag, the differential equations of motion of seed particles in a two-dimensional swirling flow, expressed in cylindrical terms, with a prescribed swirl velocity, V_θ, and radial velocity, V_r, are given by

$$\frac{dV_{r_P}}{dt} = \frac{V_{\theta_P}^2}{r} + \frac{1}{\tau_v}(V_r - V_{r_P})$$

$$\frac{dV_{\theta_P}}{dt} = -2\frac{V_{\theta_P} V_{r_P}}{r} + \frac{1}{\tau_v}(V_\theta - V_{\theta_P})$$

where P denotes particle values (**23**). The time constant is $\tau_v = \rho_P d_P^2/(18\mu)$ and the equations are coupled through the Coriolis acceleration terms.

A swirling flow of this type is encountered in the tip vortex shed from a wing or helicopter rotor. In this case the seeding particles are forced outwards from the viscous core of the vortex in a manner that depends critically on the particle diameter, particle mass and the tip vortex circulation. The effect is more significant in model studies where, although the tip vortex strength (circulation) is reduced by the scale factor, the viscous core remains of the order of the blade thickness, which tends to lead to larger centripetal accelerations inside the vortex core (**24**).

1.6 Lagrangian and Eulerian descriptions of fluid motion

Historically, the measurement of flow has used point sensor systems to provide a time series of measurements at discrete positions effectively measuring the Eulerian velocity. In a Eulerian description of the flow, the independent variables which are used to characterize conditions are the spatial coordinates x, y, z and time t. PIV, however, follows the motion of tracer particles, where each is taken as representative of a local element of fluid allowing its condition to be monitored as it moves in space. This representation is essentially Lagrangian since the initial coordinates of the fluid element being followed, and the time instant, define its condition.

The spatial correlation in flow conditions may be inferred from a series of Eulerian measurements taken by a point sensor at various spatial positions, by using conditional sampling to align the time origins of the data sequences. Alternatively, the Taylor hypothesis, relating time variation to space variation of flow through the assumption of a convecting, statistically stationary, turbulent field, may be used to convert temporal velocity measurements to spatial velocity measurements (**25**). This application of the Taylor hypothesis to relate Eulerian and Lagrangian descriptions is often non-trivial as the flow may be inhomogeneous both in time and space. The stationarity of a Eulerian velocity field does not necessarily imply that the Lagrangian velocity is a

stationary random variable. This is an important feature, where the Lagrangian autocorrelation must not depend on absolute time if the Taylor method is to be valid (**26**).

The estimation of fluid velocity from PIV measurements assumes no acceleration of the seeding particle during the flight from the first image capture position to the second image capture position; i.e. the velocity magnitude and direction are constant. Where acceleration takes place the initial and final positions of the object particle are obtained from

$$\Delta x_{\mathrm{P}} = x_{\mathrm{P}}(t + \Delta t) - x_{\mathrm{P}}(t) = \int_{t}^{t+\Delta t} v_{\mathrm{P}}(t)\,\mathrm{d}t$$

The velocity obtained from the flow-following particles is implicitly Lagrangian while the assumption is often made that Eulerian velocities are measured. Studies have been made where the Lagrangian statistics have been estimated directly from PIV measurements (**27**, **28**).

2 METHODS FOR ANALYSING PIV IMAGES

2.1 Young's fringe analysis method

The method of image analysis initially adopted in speckle and high image density PIV was that used in speckle metrology. An 'interrogation' region of the double-exposure image (transparency) of the flow was illuminated by a low-powered laser beam. The image pairs acted as interfering point sources, with the transmitted light forming Young's fringes. The transparency and the plane on which the fringes were being observed were arranged to be in the principal focal planes of a converging lens, so that the fringe pattern was an accurate Fourier transform of the phase and the amplitude of the transmitted light from the interrogation region (**29**) (Fig. 4). The amplitude and orientation of the fringe spacing was used to infer the image displacements.

Linear direction searching methods were, at first, used to determine fringe direction. The intensity of the fringes was then digitally integrated along their length, so reducing the measurement problem to a single dimension (**30**). Some used a cylindrical lens to reduce the fringe pattern to a one-dimensional intensity pattern prior to digitizing (**31**), while other impressive early work demonstrated that Young's fringes could be obtained from in-line holograms (**32**). The signal-to-noise ratio obtained in this form of analysis was improved by first contact printing the PIV transparency (**14**).

The fringe pattern also contains particle size information which can be obtained from the intensity halo, while the fringe visibility can be directly related to the flow variability (**33**, **34**).

2.2 Correlation methods

2.2.1 Autocorrelation

A Fourier transformation of the fringe pattern produced by coherent illumination of a PIV flow scene transparency produces the spatial autocorrelation function

$$R_{xx}(\boldsymbol{r}_{\mathrm{d}}) = \int I(\boldsymbol{r}) I(\boldsymbol{r} + \boldsymbol{r}_{\mathrm{d}})\,\mathrm{d}\boldsymbol{r}$$

of the transmitted light intensity, I, where $\boldsymbol{r}$ is the measured position in the film plane and $\boldsymbol{r}_{\mathrm{d}}$ is the displacement vector between the members of an image pair. The autocorrelation also contains noise due to film grain effects, electronic noise and spurious particle pairing.

The resulting autocorrelation function of a double-exposure PIV image has a zero-order (self-correlation) peak at the origin and two first-order peaks at displacements of plus and minus the displacement between particle images (Fig. 4). Peaks also occur due to random correlation between adjacent particle images from independent particle pairs. In order to minimize the possibility of choosing the wrong peak in the autocorrelation function, the ratio of the second-tallest peak to the tallest peak is used to validate the selection by acting as a variable threshold operator. The velocity is then obtained by measuring the distance between the centroids of the zero-order and the first-order peaks. The expectation value of the velocity obtained in this way is a volume average of the velocity in the interrogation cell (**35**), namely

$$\langle \boldsymbol{v}_{xx} \rangle = \frac{\int u(\boldsymbol{r}, t) W\,\mathrm{d}\boldsymbol{r}}{\int W\,\mathrm{d}\boldsymbol{r}}$$

where $\boldsymbol{r}$ is the displacement measured in the object (flow) plane and with W being a weighting function which takes into account the temporal and spatial variation in illumination intensity.

2.2.2 Cross-correlation

This method can be used in analysing single-frame, double- or multiple-exposure PIV images (**36**). In a single-frame analysis the correlation is conducted between a first window and second window in the image. The second window position is chosen from a local estimate of the mean velocity obtained, for instance by an autocorrelation procedure. The second window is larger than the first so that the probability of unpaired images is reduced and the signal-to-noise ratio increased (**37**) (Fig. 4).

Cross-correlation may also be used if the images recorded by each exposure can be separately identified. For example, adaptive optics have been used to modify the point-spread function of the recording system in such a manner that spatial filtering can be used to address the images recorded by each exposure (**38**).

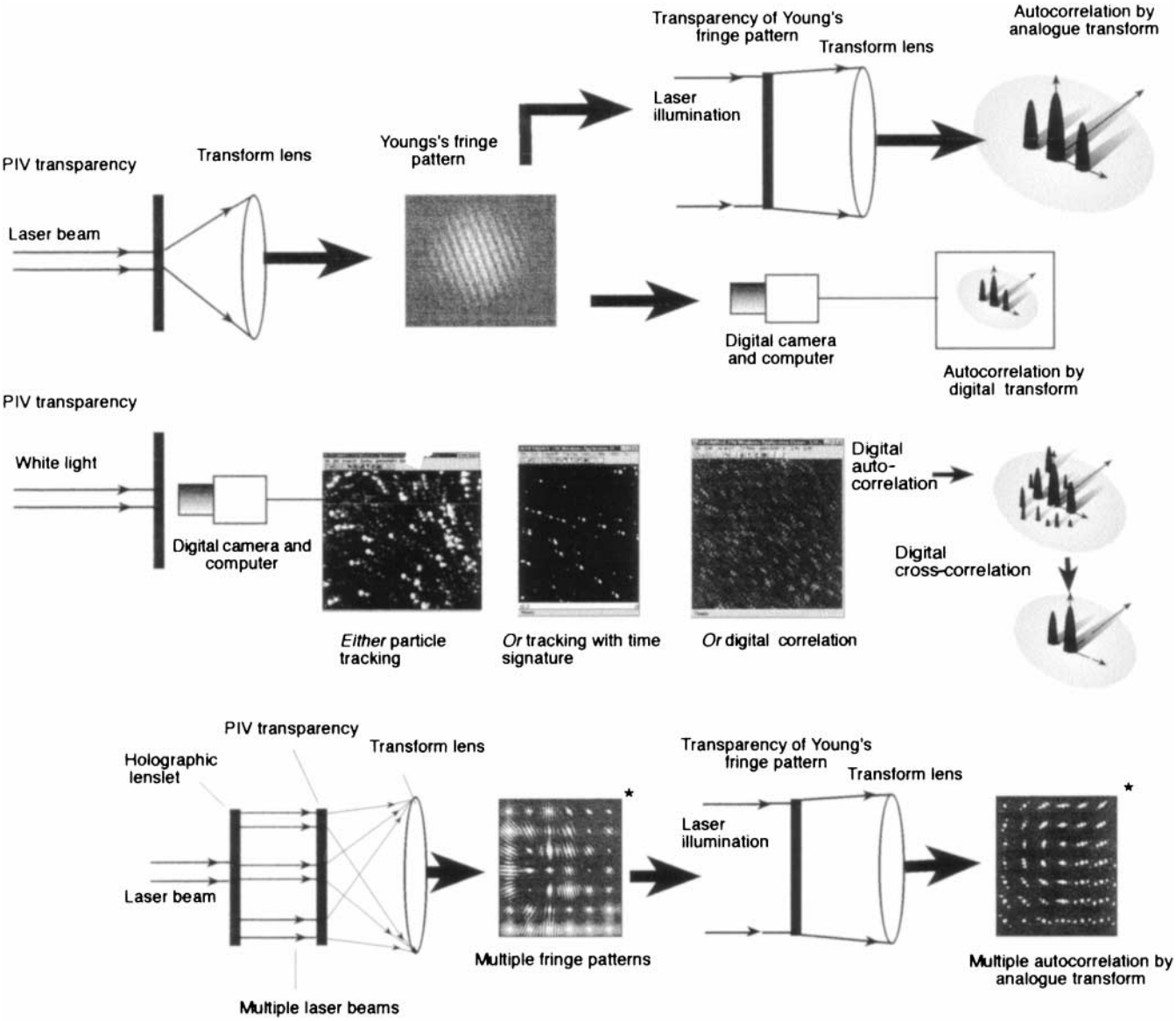

Fig. 4 Schematic diagram of PIV transparency analysis methods. [The images marked * are taken from reference (**4**). Reprinted with permission]

A novel alternative to image correlation has been proposed which views the initial particle images as interconnected sprung masses which undergo a constrained perturbation to take up their final positions. Using optimization arguments a match between the particle groups is achieved (**39**).

2.2.3 Optical correlation analysis

The efficiency of the optical transformation method has encouraged the development of fully analogue processing. In this style of analysis a further analogue Fourier transformation of the *amplitude* of Young's fringes is implemented, producing the autocorrelation of the particle image displacements (Fig. 4). This can be implemented by recording Young's fringes photographically. The ingenious use of a holographic lenslet to produce multiple interrogation beams, and thus fringe patterns, then makes photographic analogue processing efficient (**40**) (Fig. 4).

The commonest approach in analogue processing has been to use an electro-optical stage to measure the intensity of Young's fringes, convert the distribution to amplitude and then transmit the information as amplitude and phase. The transmitted optical data are passed through a second optical transformation, forming the required autocorrelation function. Photorefractive crystals have been used in constructing such analogue transformation systems to achieve this end (**41**, **42**). Others have used liquid crystal arrays and a Faraday effect spatial light modulator to achieve similar effects (**43**, **44**) (Fig. 5). Improvements in the hardware used in optical

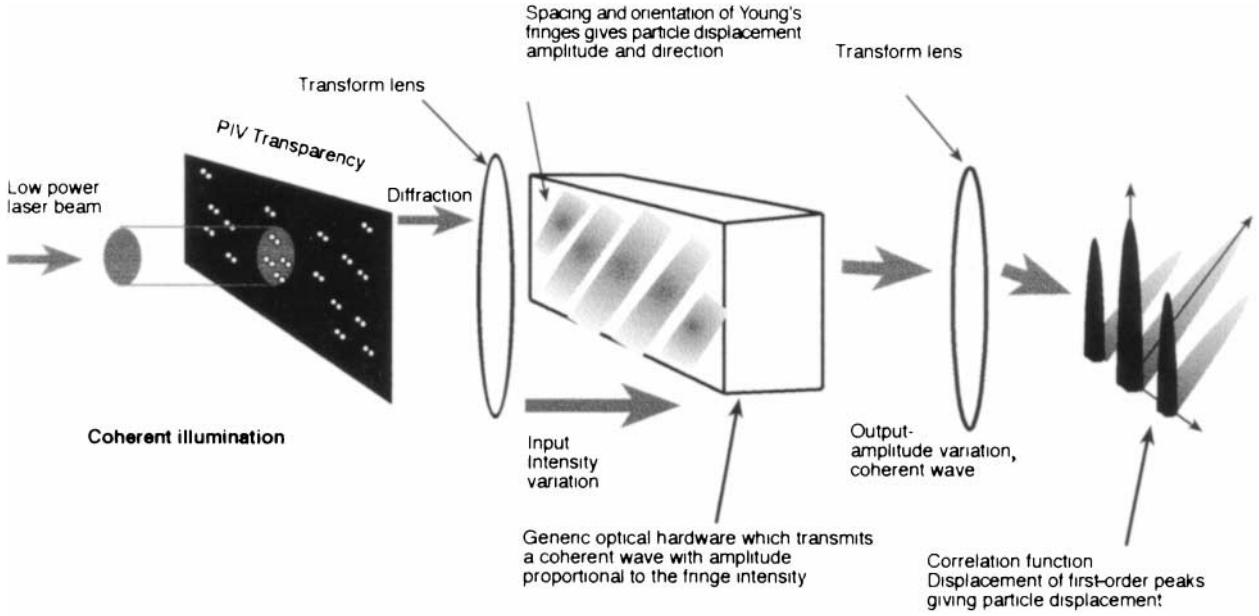

Fig. 5 The optical correlator

correlation have recently concentrated on rapid transparency scanning using a high-speed optical addressing system and increasing the analysis speed by using a parallel optical spatial autocorrelator (**45**).

Dedicated analogue analysis hardware has the potential for significant increases in processing speed provided the resources are available to install and maintain specialist hardware. However, with recent immense improvements in processing power and substantial reductions in costs of desk-top computing, digital processing continues to be the most commonly adopted approach in PIV image analysis at this time (**46**).

2.3 Spatial filtering techniques

The passage of a low-powered laser through a PIV transparency results in a diffraction pattern consisting of the two-dimensional spatial frequency spectrum of the image transmittance function. Equal velocity regions can be selected by applying a mask filter to the diffraction pattern. The reconstruction of the image by inverse analogue transformation then leads to contours of equal velocity being observed in the image space (**47**, **48**). A similar outcome can be achieved using convolution filtering (**49**).

2.4 The analysis of low image density PIV images

Low image density PIV transparencies may be processed by individual particle images being identified and tracked. The interrogation window is illuminated by an incoherent light source, and the image region then digitized and subjected to processing and filtering algorithms to improve image quality as a precursor to the evaluation of particle velocity. The velocity measurement procedure usually consists of a statistical algorithm to establish the distribution of displacements of the particle images. This information is then used in identifying the particle image pairs or groups (**50**, **51**) (Fig. 4).

2.5 Velocity bias

Velocity variations occurring within the measuring volume may result in a bias in the measured average velocity towards lower values. This is due to the reduced chance of image pairs being obtained as the velocity becomes larger, with the particle being more likely to fall outside the illuminated region during the second exposure.

Velocity bias can be reduced by a careful choice of interrogation region size relative to the average image displacement. Four experimental criteria can be used to optimize the performance of the double-pulsed autocorrelation technique (**52**). These are

(a) $N_I > 10$–20 (selecting high image density);
(b) $(u^2 + v^2)^{1/2}\,\Delta t < d_{int}/4M$, where u, v are the two in-plane velocity components, d_{int} is a dimension characteristic of the interrogation region and Δt is the time between exposures (minimizing the chance of non-pairing due to the second image lying outside the interrogation area);
(c) $w\,\Delta t < \Delta z/4$, where w is the out-of-plane velocity component, Δt is the time between exposures and Δz is the sheet thickness (minimizing the chance of

non-pairing due to movement normal to the light sheet); and

(d) $|\Delta u|/|u| < 0.2$, where Δu is the variation in velocity in the interrogation volume due to spatial gradients (reducing the velocity variation).

In high image density PIV velocity bias is not generally a problem since the ratio of unpaired images to paired images is small. Low image density PIV is much more likely to experience bias effects if care is not taken to optimize the experimental parameters. The approach used in low image density PIV particle tracking facilitates, however, the use of statistical routines to monitor any such effect.

2.6 Automated validation

Neighbourhood comparisons with other vectors or a judgement made on the basis of an *a priori* knowledge of the flow are often used to eliminate erroneous vectors in automated, post-processing, validation. Comparative methods typically consider the use of local mean, global mean or local median vector values as a means of judging vector validity (**53**).

Recent work on neural network methods has demonstrated that the different cognitive layers of the net can use information about both the global and local flow conditions in adaptively validating the velocity amplitude and direction (**54**). The neural network is also effective as a filter if overlapping particle images occur (**55**) and in fringe analysis (**56**).

In both high and low image density studies the need to interpolate data on to a regular, or body-fitted (**57**), grid is common for comparison with computational fluid dynamics (CFD) and so that derived quantities such as vorticity can be obtained.

2.7 Directional ambiguity and its resolution

2.7.1 *Image shifting*

One method of resolving the implicit 180° directional ambiguity in PIV is to apply a constant displacement on the second of the particle images pairs. This may be achieved by use of a rotating mirror viewing system (**58**–**60**) to observe the flow. Two important consequences which can result from appropriate choice of image shifting displacement are the elimination of mean flow directional ambiguity (positive image shifting) and an increase in the resolution available for measuring turbulent fluctuations (negative image shifting) (**61**). If cross-correlation is being used for image analysis, removing the mean displacement prior to the correlation operation leads to a more accurate estimate of the location of the first-order displacement peak. The shift produced is well approximated by $X_{\text{shift}} = 2\omega RM\,\Delta t$ where ω is the angular velocity of the rotating mirror, R is the distance between the light sheet and the mirror axis and Δt is the time between exposures.

A number of studies have considered higher order representation of the shift and demonstrated that errors may be generated by ignoring the effects due to the small misalignment between the illuminated (object) plane and the image plane caused by mirror deviation from the 45° orientation. The effect is to produce a viewing distortion whose magnitude is dependent on the distance from the optical axis (**62**–**64**). This effect and method of correction is similar to that used in evaluating the effect of particle motion through the light sheet (**65**).

Electro-optical devices, involving polarized illumination, have been developed in order to obtain high-velocity shifts where the shift is produced using a birefringent crystal. Difficulties may occur if significant depolarization occurs during illumination. Recent work (**66**) has shown that ferroelectric liquid crystal can be used as a polarization rotator and a birefringent element as a shifter. The system used non-polarized light and fluorescent particles (**67**, **68**) and reported rapid response times with a minimum response time of 100 μs (**66**). Image doubling using polarization has also been proposed as a means to image shift between exposures (**69**). Ambiguity resolution in digital PIV studies has been demonstrated by moving the images associated with the first pulse a known distance in pixel space (**70**).

2.7.2 *Image de-rotation*

Analogue image de-rotation may be useful when examining spinning flows produced, for instance, by impellers. De-rotation can be achieved by viewing the flow through a dove prism rotating at half the fluid spin rate (**71**, **72**). Studies have been reported combining image shifting and de-rotation (**73**).

2.7.3 *Pulse coding*

Ambiguity may be simply resolved by giving the illuminating light pulses a time signature, such as image 'tagging' (**74**, **75**). In low image density PIV studies these methods use a further statistical procedure to evaluate direction.

The use of three illumination pulses, spaced unevenly, can be combined with a triple correlation function to derive an asymmetric correlation function allowing the evaluation of the magnitude and direction of the flow (**76**). The triple correlation is defined as

$$T(i, j) = \sum_x \sum_y [S(x, y)S(x + i, y + j)S(x + ni, y + nj)]$$

where

$$n = \frac{\Delta t_{1\to 3}}{\Delta t_{1\to 2}}$$

with $\Delta t_{1\to 3}$ being the time between the first and third

light pulses and $\Delta t_{1\to 2}$ being the time between the first and second light pulses. The triple correlation function has only one first-order peak, allowing directional ambiguity to be resolved. The calculation uses direct multiplication of cross-products, leading to protracted computation times.

2.7.4 *Multiple reference beam holography*

Reference beams with different path lengths have been used, enabling a number of holograms of seed particle position to be recorded at different instants (**77**, **78**). The images can be reconstructed in a time sequence by selecting the appropriate reference beam. The images can be processed using cross-correlation methods.

2.8 Correction for viewing angle

If there is a significant flow through the light sheet then an apparent in-sheet motion is observed due to the through-sheet motion. The effect increases with increasing distance from the optical axis (**79**). A similar effect is seen when the viewing angle departs from the normal to the light sheet. If the light sheet is normal to the mean flow and the camera optical axis is oriented obliquely to the mean flow there is both a significant apparent in-plane motion due to through-sheet displacement and a variation in magnification across the field. In order to correct for these effects the following transformations are used to obtain the coordinates of the first and second object points (**65**) (Fig. 6):

$$x_1 = \frac{(d + b\cos\alpha)x_{01} - ib\sin\alpha}{\sin\alpha + i\cos\alpha}$$

$$x_2 = \frac{(d - b\cos\alpha)x_{02} - ib\sin\alpha}{\sin\alpha + i\cos\alpha}$$

$$y_1 = \frac{d - r_1\sin(\alpha - \beta_1)}{i} y_{01}$$

$$y_2 = \frac{d - r_2\sin(\alpha + \beta_2)}{i} y_{02}$$

2.9 Resolution, precision and dynamic range in PIV

A significant variation in velocity is found in many flows of practical importance. In order to maximize the resolution and dynamic range of the particle image velocimeter under these conditions variable magnification analysis may be used. The general issues of accuracy and resolution in PIV have been widely considered as the subject has progressed (**6**, **35**, **52**, **80**–**84**). Proper orthogonal decomposition (POD) has recently been suggested as an ingenious method of error detection in PIV (**85**).

In low image density particle image velocimetry a two-step approach is used in analysis. The statistical properties of the particle image field displacements are used to obtain a mean displacement and direction. These means are used to define the centres of a search window for image pairing while some multiple of the standard deviation is used to define the window limits (**51**). In an

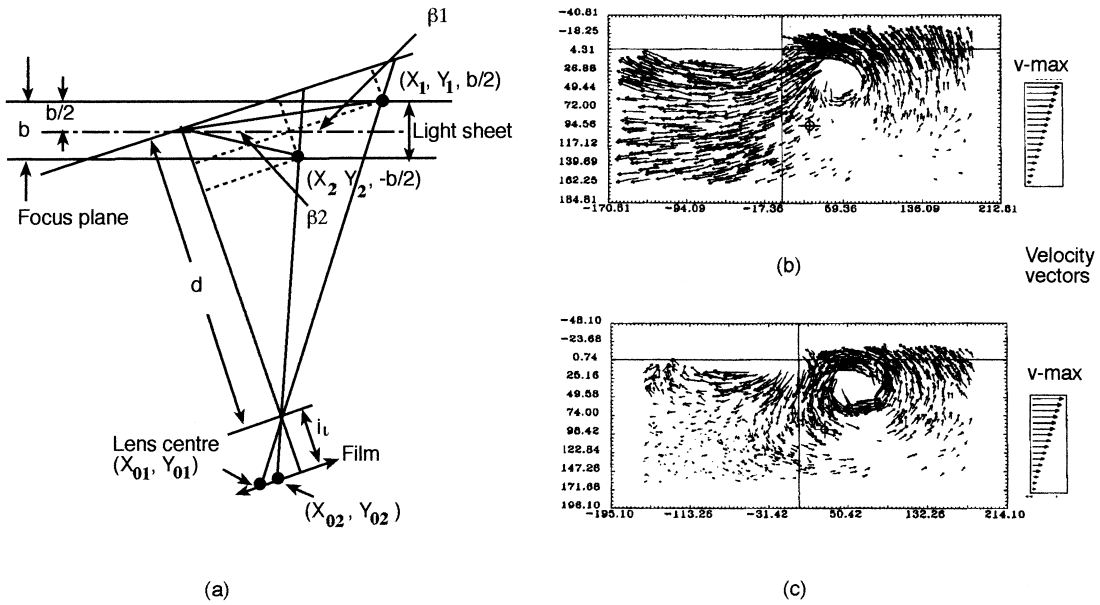

Fig. 6 The effect of the application of angle of view correction on PIV data. (a) Notation used in text. (b) Before correction and (c) after correction. [From reference (**65**). Reprinted with permission]

analogous manner recent work has applied a two-step approach to high image density PIV analysis where correlation methods first determine weighted mean displacements over the region (**86**). This local mean displacement is then used as a guide for partner searching at the individual particle image level. Two-step analysis allows the resolution to be varied, as required by the flow conditions and as permitted by the image density. Two-step analysis means that the accuracy and resolution of the analysis is no longer limited by the size of the interrogation volume in high image density studies. Efforts have been made to increase the processing speed in correlation analysis using variable-length image compression (**87**).

3 DEVELOPMENTS IN PARTICLE IMAGE VELOCIMETRY

3.1 Digital particle image velocimetry (DPIV)

The development of digital cameras of medium (512×512 pixels) to high (2048×2048 pixels and beyond) format has encouraged the development of digital particle image velocimetry (DPIV). The acquisition of PIV images in digital form eliminates the photographic stage and makes multiframe and ensemble measurements easier. The disadvantages of using DPIV are the data rates (defined by the video framing rate of 25 Hz) and the loss of spatial resolution (**88**, **89**).

In DPIV the combination of multiple pulsing and multiple framing can be used to increase the dynamic range (**90**). Frame-by-frame flow tracer cross-correlation has been applied to video images (**91**). The equations associated with the digital equivalent of Young's fringes have been formulated and investigated by numerical simulation (**36**). Numerous DPIV investigations using correlation analysis methods and tracking algorithms in engineering flows have been reported (**92**–**94**). DPIV has also found useful application in transonic flows (**95**).

3.2 High-speed DPIV

An ultra-high-speed video system has been developed for fast process monitoring (**96**) and exploited for flow measurement (**97**). The system allows exposure times down to 0.6 μs and exposure intervals of 50 ns. The system is capable of delivering up to eight frames. The camera uses a beam-splitter mirror and eight frame-grabber cards. The capture of the time series of images is controlled by the sequential release of freely triggerable electronic shutters.

The DPIV velocity field computation speed can be increased by two orders of magnitude using a video motion estimation processor (MEP) chip (**98**). The method of computation differs from the correlation approach in that, instead of summing the product of the image intensities, the MEP sums the absolute value of their difference.

3.3 Cinematic PIV

PIV studies using cinematic recording have allowed information regarding both the temporal and spatial evolution of the flow fields to be obtained. Early related work used shadowgraphs recorded as high-speed motion pictures which were digitally analysed to investigate fluid mixing (**99**). A high-speed drum camera has been used to conduct time-resolved PIV studies in low seeding density conditions (**100**). Recent work in the high seeding density regime used the cinematic PIV method to obtain high-resolution measurements in a free shear layer (**101**). Using a laser scanning system synchronized with the camera enabled the capture of three images for each particle per frame with a consequent improvement in the signal-to-noise ratio in the correlation plane.

3.4 Three component methods

No universal scheme for three velocity component measurements has so far been adopted. Methods used all have considerable experimental and processing difficulties. Most approaches may be classified as stereographic (**102**), holographic (**103**), multiple-plane (light sheet) (**104**) in methodology, with some studies combining the techniques (**105**).

3.4.1 Stereogrammetry

Stereogrammetry requires the precise matching of equivalent views in images obtained from two, or more, viewpoints. In PIV the three components of velocity can only be determined when the relative positions of the viewpoints (camera parameters) and the laser sheet are known so that a transformation matrix relating world (object) coordinates to film (image) coordinates can be derived (**106**). Additionally the views need to be recorded simultaneously.

The stereogrammetry lateral observation system (Fig. 7c) utilizes two adjacent, identical, cameras, C_L and C_R, with parallel optical axis. The centres of the two image planes are O_L and O_R. The relationships between the object point, $P(X, Y, Z)$, and the corresponding images on the two film planes are

$$x_R = \frac{X - d}{Z} i, \qquad x_L = \frac{X}{Z} i$$

$$y_R = y_L = \frac{Y}{Z} i, \qquad Z = \frac{i}{x_L - x_R} d$$

where i is the distance of the image plane from the lens centre, identical for the two views since the cameras are

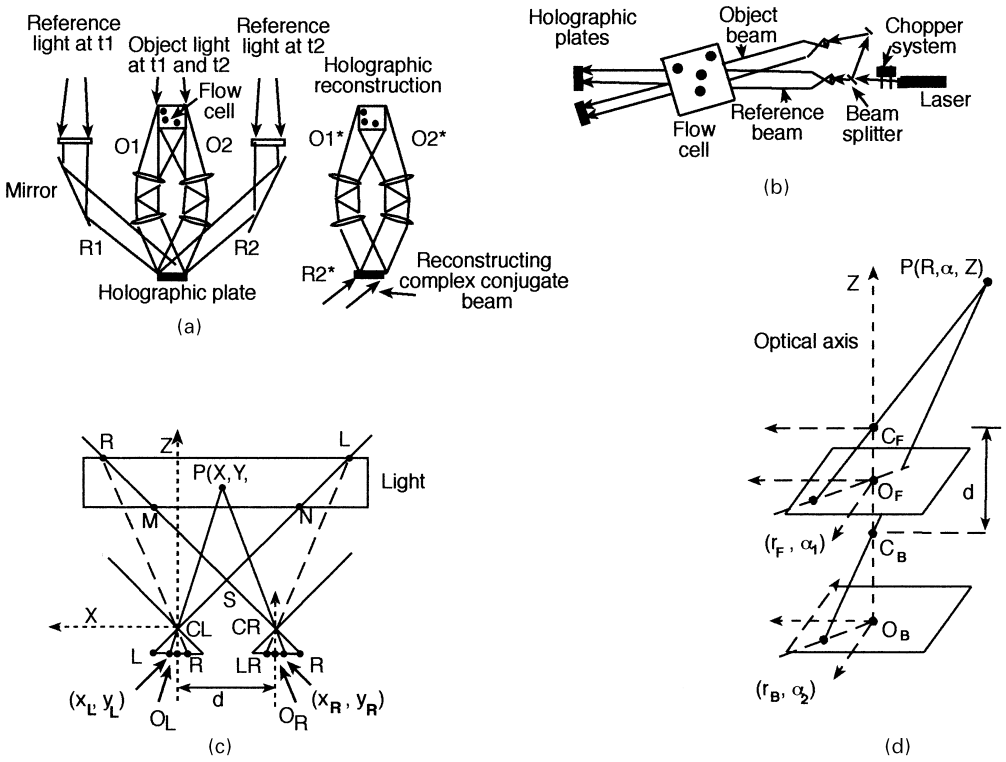

Fig. 7 (a) Off-axis double-pulse holography with two reference beams (**117**). (b) Stereo in-line holography (**105**). (c) Lateral displacement stereogrammetry and (d) axial stereogrammetry (**108**). [All reprinted with permission]

identical, and d is the camera separation. Three-dimensional measurements are only possible in the region of overlap of the two views.

View reconciliation, where corresponding image segments in the two views are matched to identify areas representing identical regions of the object volume, is non-trivial. Difficulties may occur as there is not necessarily an unambiguous match. In practice the procedure is to search the possible corresponding areas in the two views to identify common features. An example of early PIV work used semi-manual reconciliation of stereo views of the motion of helium bubbles in a vortex wake (**104**).

The axial stereo system for stereogrammetric observation is less liable to suffer from the correspondence matching ambiguities (**108**) (Fig. 7d). In practice a beam splitter is used to avoid obstruction of view of one camera by the other. The camera lens centres are located at C_F and C_B on the optical axis. The real-world coordinate system is taken as cylindrical with the origin at C_F and the Z axis is coincident with the optical axis. The relationships between the real-world point $P(R, \alpha, Z)$ and its images (r_F, α_1) and (r_B, α_2) are

$$\frac{r_B}{i_B} = \frac{R}{Z + D}, \qquad \frac{r_F}{i_F} = \frac{R}{Z}$$

$$\alpha_1 = \alpha_2 = \alpha$$

or

$$Z = \frac{r_B i_F}{r_F i_B - r_B i_F} d, \qquad R = \frac{r_F r_B}{r_F i_B - r_B i_F} d$$

where i_F and i_B are the image distances from the respective image planes to the corresponding camera lens centres. The two cameras have different magnifications but corresponding image points are found at the same azimuthal angle in the two images. The fact that the search range for the corresponding features along the radial line is much smaller than in the lateral viewing system makes the reconciliation much simpler. In-line stereogrammetry gives an increasing resolution with distance from the optical axis. An *in situ* calibration may be implemented which uses an optical calibration grid placed in the laser sheet to determine the relationship between the views and object space.

Variants of the stereoscopic method have been reported where a single camera was used in a split-screen arrangement to obtain multiple views and compared with the performance of in-line holography (**105**). A stereo interpretation method has been developed where the three-dimensional tracks of particle images were matched automatically (**109**). Another ingenious processing method to aid view reconciliation uses back-projection of the *in situ* particle images into object space

(**110**). The stereoviewing method has been applied to size and velocity measurements in two-phase flows with careful consideration being given to particle responsiveness in the analysis (**111**).

Stereoscopic DPIV using electronic mixing of the output of two video cameras storing the two views on a single frame has been reported (**75**). Recent advances in electronic camera systems have led to their use in a number of studies (**110**, **112**). The general relative inaccuracy of the out-of-plane measurements compared with the in-plane measurements has been demonstrated (**80**).

3.4.2 Holographic PIV (HPIV)

The use of holography in PIV enables the measurement of three components of velocity, throughout a volume of the flow, to be obtained (**103**). Multiple reference beam holographic methods have been used to record different planes in the flow. HPIV has used both in-line (Gabor) holography and off-axis or Leith–Upatnieks holography (**113**–**115**). Holographic film has a much higher resolution than that commonly used in PIV and consequently more scattered light from the particles is needed to obtain a satisfactory image.

Off-axis holography is susceptible to errors resulting from vibration, noise or inaccurate reproduction of the reference beam at the reconstruction stage. Consequently, the in-line method, using forward scattering, has been favoured in many studies (**105**). A single laser beam passes through the seeded flow region, with the reference beam consisting of the unscattered light while light scattered from seeding particles comprises the object beam. The interference pattern of these two beams is recorded on a holographic plate. Three-dimensional information can be obtained from the reconstructed image by using observation optics with a shallow depth of field. Traversing the viewing system along the optical axis allows in-focus particle images to be identified in three-dimensional space. This approach can be improved by recording two holographic images, obtained from different viewpoints simultaneously, and then combining holographic reconstruction with stereogrammatical viewing, allowing a three-dimensional reconstruction of the flow scene with a wide angle of view (**101**, **116**). Improvements in image quality have been reported using the phase conjugate play-back geometry to obtain a real holographic image on reconstruction and to compensate for aberrations produced by the imaging and viewing systems (**117**).

The off-axis method uses separate optical paths for the object and reference beams and requires a more elaborate set-up. The advantage of the off-axis system is that the independence of the reference and object beams allows the intensity of the image and object beams to be equalized by separate adjustment, leading to improved hologram quality. Using relay optics it has been shown possible to collect the light scattered from the particles in two near-forward directions. This allows the recording of the holograms at two independent time instants using two reference beams. The reconstructed images can be interrogated in three dimensions and by tracking the interrogation region in the reconstructed image it should be possible to produce a three-dimensional autocorrelation function (**118**) (Fig. 7).

A hybrid HPIV system has been reported which uses both in-line and off-axis configurations offering an improvement in signal to noise and dynamic range (**119**). High-quality holography studies have made an important contribution in the understanding of transonic flows (**120**).

3.4.3 Image properties

Using two parallel light sheets of different colours, an indication of the cross-sheet motion can be obtained from an inspection of the colour of the images (**121**, **122**). Alternatively, the intensity distribution across the laser sheet may be used as a means of determining particle location by relating the image brightness to its position in the sheet (**123**). The dependence of brightness on other factors, such as particle size or reflectivity, means that procedures using this approach need careful interpretation. The out-of-focus image size may be used as a depth indicator (**124**), as can the size and shape of the point spread function from coded apertures (**125**). High-speed movie recording of PIV scenes has enabled the estimation of the out-of-plane component by arguments of continuity (**126**).

3.4.4 Multiple-sheet methods

Tomography is a quasi-three-dimensional measurement technique which represents three-dimensional space from a series of images taken in parallel planes distributed along the third axis. Recent work has used multiple-beam holographic recording to obtain high-quality tomographic measurements in high-speed turbulent flows (**127**). A multiple-sheet method has been suggested (**128**) which looks at the magnitude of the correlation peak from single-sheet measurements as a means of estimating out-of-plane motion. In order to eliminate other influences a second light sheet was used for normalization purposes. It is also feasible to make out-of-plane velocity measurements by spatial cross-correlation of particle images lying within parallel light sheets.

3.4.5 The use of colour in PIV

Colour-coded streaklines can be used to make velocity and acceleration measurements (**129**) while a three-colour system enabling directionally unambiguous measurements to be obtained has been demonstrated (**130**). Synchronous coloured illumination (partially overlapping, parallel light sheets of different colours, pulsed simultaneously) allows the out-of-plane motion

(**131**) to be estimated using colour coding. Asynchronous coloured illumination (overlapping, parallel light sheets of different colours, pulsed sequentially) has been used to obtain particle image pairs of different colours joined by a streak of a third colour. The streak eliminates erroneous pairing and directional ambiguity is resolved using the colour coding.

A twin-cavity Nd:Yag laser, with one of the output beams used to pump a dye laser followed by a beam combination utilizing dichroic optics, has found common application (**132**), with both colour film (**133**) and twin-coloured cameras being used (**134**, **135**).

3.5 Hardware developments

3.5.1 Laser scanners

Beam sweep (speckle or particle image) velocimetry uses either a scanning galvanometer (**136**) or a rotating multifacet prism (**137**) to periodically sweep a continuous wave (CW) laser beam through a plane in the flow. The beam is not interrupted by a chopper or gate so more light is delivered to the flow and the effective illumination level is much higher. This is advantageous where laser power is a limiting factor (**138**), though mechanical considerations limit the general applicability to low-speed flows. In an effort to extend the method to higher speed flows a dual-beam system has been reported in which a CW laser was split into two beams that had slightly different angles of incidence on the prism scanner (**137**). The result was a dual sweep of two laser beams through the fluid for each facet of the prism. The system was found to be suitable for flows with speeds up to 15 m/s. A mirror scanning system sweeping beams of different colours has been devised to allow the resolution of the flow image directional ambiguity (**139**, **140**). Systems comprising a helical array of mirrors on a drum have been used to displace the beam prior to sheet formation (**141**, **142**) (Fig. 8). A further variation on beam sweeping has been the moving of the expanded sheet through the flow volume (Fig. 8). Studies using an oscillating mirror as a means of scanning the sheet have been conducted using this strategy (**143**, **144**) (Fig. 8). The method has many similarities to tomography and, coupled with high-speed video recording, coloured illumination and analysis incorporating the continuity equation, offers the potential for higher Reynolds number flow studies, currently limited to around $Re = 1000$ (**145**).

3.5.2 Fibre optics

In addition to off-the-shelf fibre optical systems for laser delivery, reported work has examined the possibility of delivering pulsed-laser illumination to the PIV system (**146**). Using large-core, all-silica multimode fibres a transmission pulse energy upper limit of 14 mJ was demonstrated. The system reported had relatively poor output beam quality, restricting the formulation of a well-collimated light sheet required in PIV. The intensity profile additionally may show considerable speckle-induced intensity variations which lead to degraded PIV images.

3.5.3 Laser-less PIV (image intensifier system)

Improvements in commercially available hardware have led to exciting new innovations in PIV. One of these is the laser-less DPIV system based on a high-resolution image intensifier (**147**). The CCD camera used an advanced, ultra-high-speed gated, image intensifier, monochrome video camera. The camera was controlled locally by an internal computer chip with which the PC image capture and analysis software suite could communicate. The camera could be triggered automatically by external events or by a keyboard under software control. This allowed the implementation of a flexible and

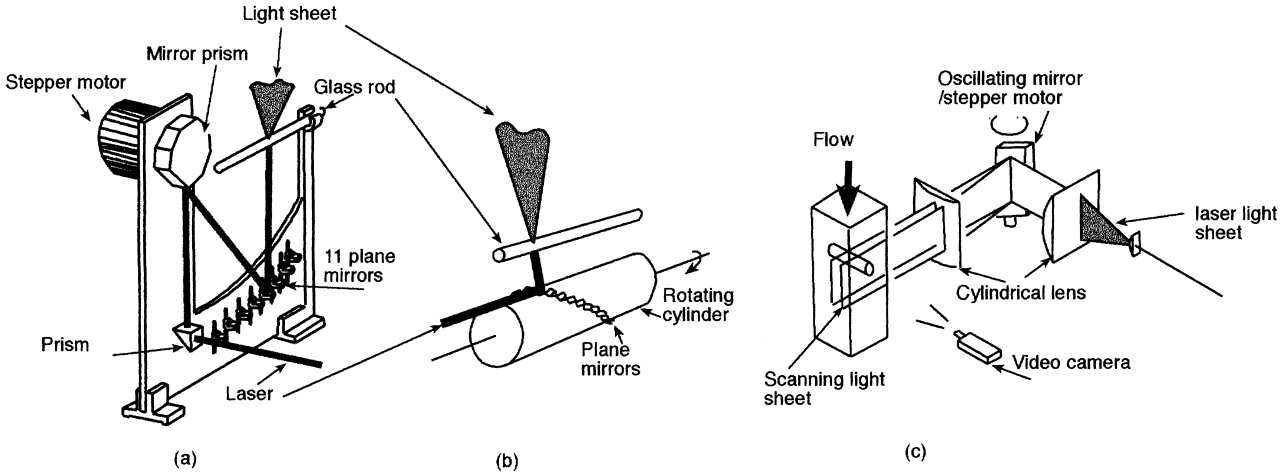

Fig. 8 Systems for laser sheet sweeping. [(a) and (b) after reference (**141**) and (c) after reference (**144**). Reprinted with permission]

cost effective DPIV system with a wide dynamic range. The image intensifier hardware and control software allowed multiple exposures, of different duration, within the same digital frame. The camera sensitivity could be software adjusted to suit different levels of illumination. This feature allowed the capture of DPIV images with embedded time signatures. Previous difficulties with resolution in image intensifier systems were overcome by direct lens coupling between the intensifier and CCD sensor array.

3.5.4 PC bus developments

The commonly used frame grabber based on the ISA (Industrial Standard Architecture) bus has always exhibited a data bottleneck due to its slow transfer rate, typically 2 Mbytes/s. This was overcome in some systems by having on-board frame storage and basic data processing, at best an expensive, incomplete solution.

Recently frame boards have appeared taking advantage of the PCI (peripheral computer interface) bus which has a higher data transfer speed, typically 45 Mbytes/s. At these speeds, the new boards are able to transfer images continuously across the bus to the PC RAM (random access memory), in real time, until the memory is exhausted. Direct display on the computer monitor using the PCI bus is now possible, eliminating the need for a separate monitor. The data memory and processing are now functions of the host computer, rather than the frame board, and can therefore take advantage of developments in PC technology without the need for new architecture boards. The new boards enable the user to define the video input format, allowing the image size configuration to be changed. This is a further significant improvement since changing the camera resolution or scan characteristics can be accommodated by reconfiguring the board at no cost.

3.5.5 Digital parallel processors

The computationally intense nature of PIV image analysis has led to various schemes for decreasing computational times using a parallel processing strategy. The early availability of the digital array processor (DAP), a dedicated parallel processor, having an array of 4096 processors linked to a host mainframe, stimulated development of software taking advantage of the advanced architecture to achieve high computational speeds (**148**). An array of eight vector processors has been used to achieve speeds of the order of one hundred vectors a second (**149**). In optimizing the performance of such systems it is essential to eliminate data bottlenecks where the processing speed is restricted by poor data communications. In this case the problem was overcome using a video camera array and a pipeline processor which passes image data to each processor to optimize its efficiency.

4 APPLICATIONS

Most areas of experimental fluid mechanics are now finding benefit from PIV diagnostic studies. In addition to velocimetry data, derived quantities, such as vorticity, acceleration (**150**) and pressure field calculations using PIV data, have been reported (**151**). Two-step processing (auto-correlation followed by cross-correlation) has been used as a means of examining spatio-temporal flow evolution. The study obtained vorticity measurements and estimates of the accuracy as a function of spatial resolution (**37**).

Wind turbine aerodynamics experiments have investigated attached rotor blade flow and the trailing tip vortices using PIV (**152**). Operational turbines, both in a laboratory setting and under field conditions (out-of-doors), have been used in these studies. These first reported outdoor PIV measurements were obtained on two rotors, the largest being 17 m in diameter with a hub height 15.5 m above the ground. A sophisticated computer control system was used to synchronize the pulsed laser illumination with the turbine motion and to control the intensity of the light pulses (Fig. 9). The hydrodynamic motion associated with waves striking off-shore platforms (**153**) and ship wakes (**154**) have been investigated. The problems of seeding, image capture and synchronization encountered in applying PIV to short-duration supersonic flows have been resolved in recently reported studies. One investigation has considered flow speeds of up to 900 m/s, characterizing scramjet combustion with supersonic conditions producing shock trains (**155**). The inherent complexity of aeronautical applications, often accompanied by unsteady effects, makes PIV an important tool for advancing this discipline.

High-quality studies have recently been conducted in rotorcraft associated studies (**156**) (Fig. 6). The transition of a laminar boundary layer on a flat plate due to the growth of small instabilities is being investigated by using PIV and POD (**157**). The nature of transition, selective growth of disturbances at particular frequencies defined by the Reynolds number, followed by turbulent bursts (**158**, **159**) leading to a fully turbulent flow (**160**), make it a challenging area of research which benefits greatly from the application of optical and PIV methods.

Combustion offers an important and challenging area for PIV implementation. The velocity fields in turbulent jets in the presence of flames have been investigated (**161**–**164**), with non-reacting and reacting cases being examined to determine the result of heat release. Other jet studies have demonstrated the simultaneous measurement of velocity and particle size. The size was measured from the intensity envelope surrounding Young's fringes (**165**). The area of application is principally an efficient gas-fired boiler design.

Using high-speed recording and high-speed pulse illumination rates offered by metal vapour lasers is

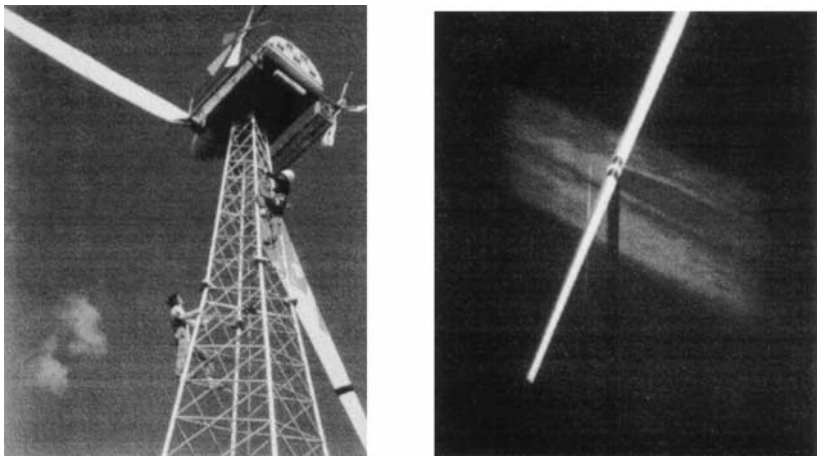

(a) (b)

Fig. 9 The first outdoor PIV experiments in 1992–3. The aerodynamics of operational wind turbines. (a) Preparing the blades. (b) The light sheet intersecting the blade. The low-power alignment beam can also be seen. [Previously unpublished. Description from reference (**152**)]

already increasing the understanding of flame swirl (**166**). Flame propagation problems offer the potential for simultaneous diagnostics using interferometry particle tracking methodologies (**167**). The air motions associated with natural convection are characterized by very low velocities and long time-scales. Studies using DPIV coupled with video recording have demonstrated the use of cinematographic velocity measurement in time-dependent natural convection (**89**). The characteristics and structure of the rear wall turbulent boundary layer are now being extensively studied using PIV (**168**) (Fig. 10). PIV studies of multiphase flows have examined the forces on bubbles entrained by a vortex using a triple exposure imaging technique that simultaneously recorded bubble velocity, fluid velocity and acceleration (**150**). A model reactor that contained three independent phases has been investigated using film and CCD cameras. The velocity and phase of the detected images was determined by image processing (**169**). Measurements made of an impinging air jet propelling solid particles have been reported (**170**), with ensemble averaging used to compute the phase-averaged conditions (Fig. 10). Smoke and droplet seeding was used to obtain qualitative and quantitative fluid phase measurements with the solid phase comprising glass beads. High-quality measurements were obtained of the fluid and particle behaviour and density (Fig. 10).

The complex flows associated with the internal combustion engine have been investigated using PIV (**171**). Characterization of the barrel swirl that occurs during the compression stroke and large-scale and small-scale structures were detected (**172**, **173**). The complex, unsteady, three-dimensional flow field associated with the pump impeller and its vaned diffuser has been investigated using a combination of PIV and LDA (**174**). This highly complex flow benefits from the combination of time-dependent and spatially-dependent measurements (**174**). The structure of the vortices, particularly their coherence along the cylinder axis, is fundamental in determining the unsteady loading caused by the shedding and has been widely investigated using PIV (**37**, **175**, **176**). In a careful study, PIV has been used to resolve a long-standing, fundamental controversy regarding a suspected discontinuity in the vortex strength–Reynolds number relationship in the laminar regime of the flow around a cylinder (**177**). The use of PIV for flow measurements in model heart pumps especially near heart valves has been reported (**178**, **179**). The availability of thermochromic liquid crystals has encouraged investigation where colour CCD recording has enabled the crystals to act as flow tracers and temperature sensors, for example in heat exchanger studies (**180**).

There has been considerable interest in the application of PIV to the fluid mechanics of the marine environment. Small-amplitude gravity waves (**181**), breaking waves (**182**) and the interaction of waves and current (**183**) and breakwaters (**184**) have all received attention in recent years. The subject continues to attract attention. In an impressive series of early experiments the wake of the flight of the pigeon, the jackdaw and the kestrel have been investigated using stereoscopic PIV (Fig. 10). The trained birds flew through a cloud of helium bubbles and the resulting bubble motion, illuminated by a white light flash system, captured the motion of the shed vorticity from the birds' wings (**107**).

5 CONCLUSIONS HIGHLIGHTING AREAS OF FUTURE DEVELOPMENT

PIV has developed into an effective measurement method, its evolution having been the principal activity

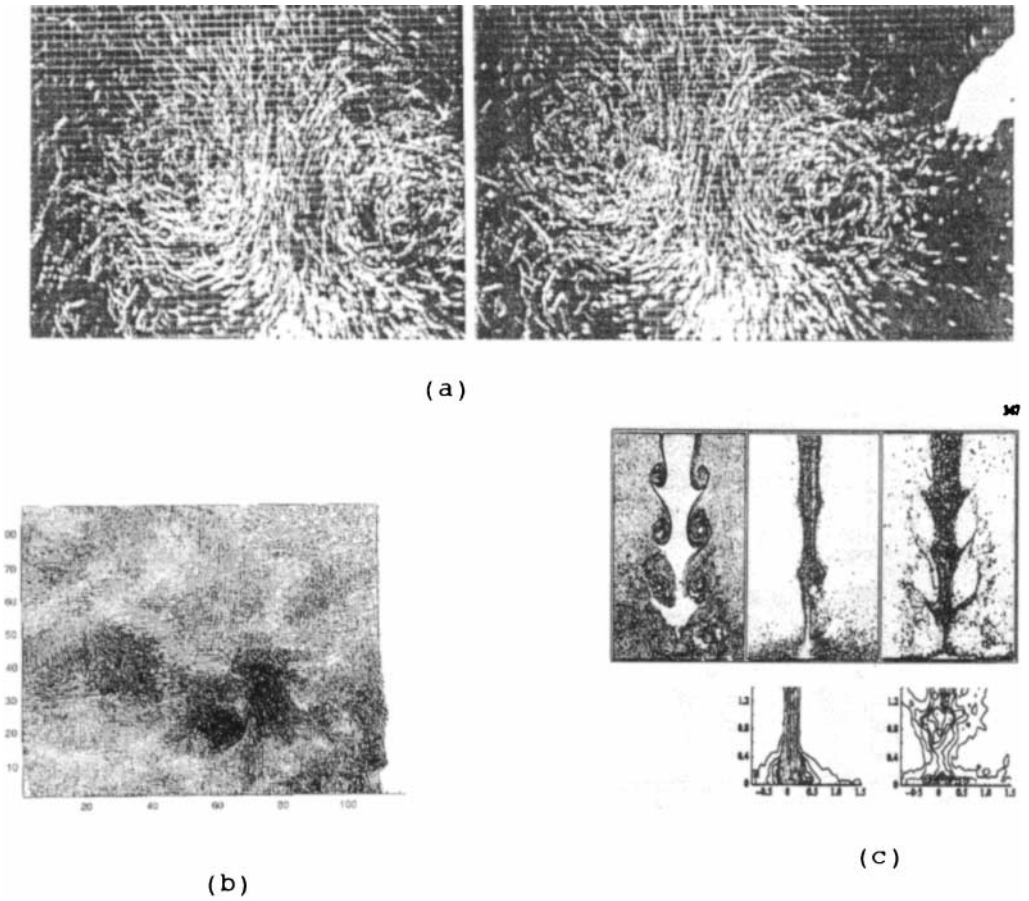

Fig. 10 Applications of PIV. (a) A stereoscopic PIV image pair showing the wake of a pigeon in flight. [From reference (**107**). Reproduced with permission.] (b) PIV velocity vector field in a streamwise-normal plane of a sudden expansion in a pipe flow. [From reference (**86**). Reproduced with permission.] (c) An impinging air jet. [From reference (**170**). Reproduced with permission]

of a number of laboratories over the last twenty years. The method is now well established with its limitations and strengths being understood and well documented, as indicated in the many referenced papers in this article and elsewhere (**3**–**8**).

Considerable efforts are still being made to increase the processing speed of PIV images using ingenious software and complex hardware. Meanwhile, complementary developments of experimental methods, such as stereogrammetry and HPIV, are increasing the complexity of the images to be analysed. This is an area where there will be sustained development over the coming years.

PIV is being successfully used to aid, both qualitatively and quantitatively, the understanding of turbulence (**185**), where the presence of coherent structures has long seemed, tantalizingly, to hold the key to a general understanding of this most complex of phenomena. PIV is well suited to pursue this end.

Complementary developments in electronic, hyperjournal publishing on the world wide web (www) now offers the possibility to present PIV animations (**186**) and digitized video records of laser sheet visualization (**187**) alongside the written word. This possibility, given the near-universal accessibility of the www, will undoubtedly accelerate the exchange of ideas and understanding of complex fluid motion.

An important supporting relationship has developed between computational fluid dynamics (CFD) and PIV. The provision of velocity data, obtained simultaneously, on a distributed spatial grid from PIV studies has led to considerable interest in using the data to validate CFD codes. In a reciprocating manner, many investigators developing PIV analysis systems have looked to CFD as a means of calibrating and validating their analysis software by introducing 'virtual' particles into a numerical flow model and attempting to reconstruct the flow from the resulting trajectories or images (**188**).

The need to understand the processes of complex fluid behaviour are reflected in the many sponsors of PIV research, with interests coming, for example, from environmental agencies, automobile and aircraft manufacturers, energy producers and defence agencies. The importance of PIV as a measurement tool is well recog-

nized and seems likely to continue to find application in stimulating areas of fluid mechanics research.

REFERENCES

1 **Merzkirch, W.** *Flow Visualisation*, 1987 (Academic Press, New York).
2 **Lauterborn, W.** and **Vogel, A.** Modern optical techniques in fluid mechanics. *Annual Rev. of Fluid Mechanics*, 1984, **16**, 223–244 [reprinted in reference (**6**)].
3 **Adrian, R. J.** Particle-imaging techniques for experimental fluid mechanics. *Annual Rev. of Fluid Mechanics*, 1991, **23**, 261–304 [reprinted in reference (**6**)].
4 **Hinsch, K. D.** Particle image velocimetry. In *Speckle Metrology* (Ed. R. S. Sirohi), 1993, Ch. 6, pp. 234–324 (Marcel Dekker, New York, Basel, London).
5 **Buchave, P.** Particle image velocimetry. In *Optical Diagnostics for Flow Processes* (Eds L. Lading *et al.*), 1994 (Plenum Press, New York).
6 **Grant, I.** (Ed.) *Selected Papers on PIV; SPIE Milestone Volume MS99*, 1994 (Society of Photo-Optical Instrumentation Engineers, Bellingham, Washington).
7 **Adrian, R. J.** Bibliography of particle velocimetry using imaging methods: 1917–1995. TAM Report 817, UILU-ENG-96-6004, University of Illinois, Urbana, 1996.
8 **Grant, I.** Particle image velocimetry. In *Optical Measurement Techniques and Applications* (Ed. P. Rastogi), 1997, Ch. 11 (Artech House Books, Boston, London).
9 **Archbold, E.** and **Ennos, A. E.** Displacement measurement from double-exposure laser photographs. *Optica Acta*, 1972, **19**(4), 253–271 [reprinted in reference (**6**)].
10 **Barker, D. B.** and **Fourney, M. E.** Measuring fluid velocities with speckle patterns. *Optics Lett.*, 1977, **1**(14), 135–137 [reprinted in reference (**6**)].
11 **Gore, R. A.** and **Crowe, C. T.** Effect of particle size on modulating turbulent intensity. *Int. J. Multiphase Flow*, 1989, **15**(2), 279–285.
12 **Jacquot, P.** and **Rastogi, P. K.** Influence of out-of-plane deformation and its elimination in white light speckle photography. *Optics and Lasers in Engng*, 1981, **2**, 35–55.
13 **Adrian, R. J.** Scattering particle characteristics and their effect on pulsed laser measurements of fluid flow; speckle velocimetry vs particle image velocimetry. *Appl. Optics*, 1984, **23**(11), 1690–1691 [reprinted in reference (**6**)].
14 **Pickering, J. D.** and **Halliwell, N. A.** Speckle photography in fluid flows: signal recovery with two-step processing. *Appl. Optics*, 1984, **23**(8), 1128–1129 [reprinted in reference (**6**)].
15 **Born, M.** and **Wolf, E.** *Principles of Optics*, 1970 (Pergamon, Oxford).
16 **Marrett, J.** *Techniques of Modern Photography*, 1967 (Evans Bros., London).
17 **Offutt, P. W.** Development of experimental technique and studies of spatial structure in turbulent thermal convection. PhD thesis, University of Illinois, Urbana, Illinois, 1995.
18 **Adrian, R. J.** and **Yao, C. S.** Pulsed laser technique application to liquid and gaseous flows and the scattering power of seed materials. *Appl. Optics*, 1985, **24**, 44–52 [reprinted in reference (**6**)].
19 **Eaton, J. K.** and **Fessler, J. R.** Preferential concentration of particles by turbulence. *Int. J. Multiphase Flow*, 1994, **20** (Suppl. 1), 169–209.
20 **Mei, R.**, **Adrian, R. J.** and **Hanratty, T. J.** Particle dispersion in isotropic turbulence under Stokes drag and Basset force with gravitational settling. *J. Fluid Mechanics*, 1991, **225**, 481–495.
21 **Tedeschi, G.** and **Menon, R. K.** Frequency response of solid particles in oscillating flows. In Proceedings of Eighth International Symposium on *Application of Laser Techniques to Fluid Mechanics*, Lisbon, 1996, paper 12.2.
22 **Saffman, P. G.** The lift on a small sphere in a slow shear flow. *J. Fluid Mechanics*, 1965, **22**(2), 385–400.
23 **Fuchs, N. A.** *The Mechanics of Aerosols*, 1964 (Pergamon Press, Oxford).
24 **Leishman, J. G.** Seed particle dynamics in tip vortex flows. *J. Aircraft*, 1996, **33**(4), 823–825.
25 **Taylor, G. I.** The spectrum of turbulence. *Proc. R. Soc. Lond.*, 1938, **A164**, 476–490.
26 **McComb, W. D.** *The Physics of Turbulence*, 1990 (Clarendon Press, Oxford).
27 **Cenedese, A.** and **Querzoli, G.** PIV for Lagrangian scale evaluation in a convective boundary layer. In *Flow Visualisation*, Vol. VI (Eds Y. Tanida and H. Miyashiro), 1995, pp. 863–867 (Springer-Verlag, Berlin).
28 **Siu, Y. W.**, **Taylor, A. M. K. P.** and **Whitelaw, J. H.** Lagrangian tracking of particles in regions of flow recirculation. In Proceedings of First International Conference on *Flow Interaction*, Hong Kong, 1994, pp. 330–333.
29 **Goodman, J. W.** *Introduction to Fourier Optics*, 1968 (McGraw-Hill, London, New York).
30 **Robinson, D. W.** Automatic fringe analysis with a computer image-processing system. *Appl. Optics*, 1983, **22**(14), 2169–2176 [reprinted in reference (**6**)].
31 **Yao, C.-S.** and **Adrian, R. J.** Orthogonal compression and 1-D analysis technique for measurement of 2-D particle displacement in pulsed laser velocimetry. *Appl. Optics*, 1984, **23**, 1687–1689.
32 **Malyak, P. H.** and **Thompson, B. J.** Particle displacement and velocity measurement using holography. *Opt. Engng*, 1984, **23**(5), 567–576 [reprinted in reference (**6**)].
33 **Hinsch, K.**, **Schipper, W.** and **Mach, D.** Fringe visibility in speckle metrology and the analysis of random flow components. *Appl. Optics*, 1984, **23**, 4460–4462 [reprinted in reference (**6**)].
34 **Grant, I.**, **Owens, E. H.** and **Smith, G. H.** The effect of flow turbulence and interrogating beam profile on particle image velocimetry fringes. *Optics and Lasers in Engng*, 1989, **11**, 115–128.
35 **Adrian, R. J.** Statistical properties of particle image velocimetry measurements in turbulent flow. In *Laser Anemometry in Fluid Mechanics*, Vol. III (Eds R. Adrian *et al.*), 1988, pp. 115–129 (Ladoan-Instituto Superior Tecnico, Lisbon).
36 **Cho, Y. C.** Digital image velocimetry. *Appl. Optics*, 1989, **28**, 740–748.
37 **Soria, J.** An investigation of the near wake of a circular cylinder using a video-based digital cross-correlation particle image velocimetry technique. *Experimental Thermal and Fluid Science: ETF*, February 1996, **12**, 221–233.
38 **Lawson, N. J.**, **Halliwell, N. A.** and **Coupland, J. M.** Particle image velocimetry: image labelling by use of

adaptive optics to modify the point-spread function. *Appl. Optics*, 1994, **33**(19), 4241–4247.

39 **Okamoto, K., Koizumi, M., Madarame, H.** and **Hassan, Y. A.** Temporal mapping of the spring model for particle image velocimetry. In Proceedings of Eighth International Symposium on *Application of Laser Techniques to Fluid Mechanics*, Lisbon, 1996, paper 27.1.

40 **Arnold, W.** and **Hinsch, K. D.** Parallel optical evaluation of double exposure records in optical metrology. *Appl. Optics*, 1989, **28**(4), 726–729 [reprinted in reference (**6**)].

41 **Coupland, J.** and **Halliwell, N. A.** Particle image velocimetry: rapid transparency analysis using optical correlation. *Appl. Optics*, 1988, **27**(10), 1919–1921 [reprinted in reference (**6**)].

42 **Gheen, G.** and **Chen, L.-J.** Optical correlators with fast updating speed using photorefractive semiconductor materials. *Appl. Optics*, 1988, **27**(13), 2756–2761 [reprinted in reference (**6**)].

43 **Farrell, P. V.** and **Goetsch, D.** Optical analysis of particle image velocimetry data. ICALEO '89—optical methods in flow and particle diagnostics. *Proc. LIA*, 1989, **68**, 82–91 [reprinted in reference (**6**)].

44 **Kompenhans, J.**, **Reichmuth, J.** and **Hocker, R.** Data evaluation in particle image velocimetry by means of a spatial light modulator. ICALEO '89—optical methods in flow and particle diagnostics. *Proc. LIA*, 1989, **68**, 121–129 [reprinted in reference (**6**)].

45 **Mao, Z. Q.**, **Halliwell, N. A.** and **Coupland, J.** Particle image velocimetry: high speed transparency scanning and correlation-peak location in optical processing systems. *Appl. Optics*, 1993, **32**(26), 5089–5091.

46 **Huntley, J. M.** Speckle photography fringe analysis: assessment of current algorithms. *Appl. Optics*, 1989, **28**(20), 4316–4322 [reprinted in reference (**6**)].

47 **Meynart, R.** Equal velocity fringes in a Rayleigh–Bernard flow by a speckle method. *Appl. Optics*, 1980, **19**, 1385–1386 [reprinted in reference (**6**)].

48 **Palero, V.**, **Andres, N.**, **Arroya, M. P.** and **Quintanilla, M.** Fast quantitative processing of particle image velocimetry photographs by a whole-field filtering technique. *Exps in Fluids*, 1995, **19**(6), 417–425.

49 **Grant, I.** and **Qiu, J. H.** Digital convolution filtering techniques on an array processor for particle image velocimetry. *Appl. Optics*, 1990, **29**, 4327–4329 [reprinted in reference (**6**)].

50 **Agui, J. C.** and **Jimenez, J.** On the performance of particle tracking. *J. Fluid Mechanics*, 1987, **185**, 447–468.

51 **Grant, I.** and **Liu, A.** Method for the efficient incoherent analysis of particle image velocimetry images. *Appl. Optics*, 1989, **28**(10), 1745–1748 [reprinted in reference (**6**)].

52 **Keane, R.** and **Adrian, R. J.** Optimisation of particle image velocimeters, Part 1: double pulsed systems. *Measmt Sci. Technol.*, 1990, **1**, 1202–1215.

53 **Westerweel, J.** Efficient detection of spurious vectors in particle image velocimetry data. *Exps in Fluids*, 1994, **16**, 236–247.

54 **Grant, I.** and **Pan, X.** An investigation of the performance of multi layer neural networks applied to the analysis of PIV images. *Exps in Fluids*, 1995, **19**, 159–166.

55 **Carosone, F.**, **Cenedese, A.** and **Querzoli, G.** Recognition of partially overlapped particle images using the Kohonen neural network. *Exps in Fluids*, 1995, **19**, 225–232.

56 **Carosone, F.** and **Cenedese, A.** Young's fringes analysis by neural networks. In Proceedings of Eighth International Symposium on *Application of Laser Techniques to Fluid Mechanics*, Lisbon, 1996, paper 21.2.

57 **Aroussi, A.** and **Hatem, A. B.** Processing PIV images. In ASME Fluid Engineering Division, Vol. 229, 1995 Meeting on *Laser Anemometry* (Eds H. H. Huang *et al.*), Hilen Head Island, South Carolina, 1995, pp. 101–108 (American Society of Mechanical Engineers, New York).

58 **Adrian, R. J.** Image shifting technique to resolve directional ambiguity in double-pulsed velocimetry. *Appl. Optics*, 1986, **25**(21), 3855–3858 [reprinted in reference (**6**)].

59 **Landreth, C. C.**, **Adrian, R. J.** and **Yao, C. S.** Double pulsed particle image velocimeter with directional resolution for complex flows. *Exps in Fluids*, 1988, **6**, 119–128 [reprinted in reference (**6**)].

60 **Grant, I.**, **Smith, G. H.** and **Owens, E. H.** A directionally sensitive particle image velocimeter. *J. Phys. E: Sci. Instrum.*, 1988, **21**, 1190–1195; reprinted in *J. Engng Optics*, February 1989.

61 **Schlichting, H.** *Boundary Layer Theory*, 1979 (McGraw-Hill, New York).

62 **Oschwald, M.**, **Bechle, S.** and **Welke, S.** Systematic errors in PIV by realizing velocity offsets with the rotating mirror method. *Exps in Fluids*, 1995, **18**, 329–334.

63 **Raffel, M.** and **Kompenhans, J.** Theoretical and experimental aspects of image-shifting by means of a rotating mirror system for particle image velocimetry. *Measmt Sci. Technol.*, 1995, **6**, 795–808.

64 **Zhang, Z.** and **Eisele, K.** The two-dimensional velocity shift caused by the use of a rotating mirror in PIV flow field measurements. *Exps in Fluids*, December 1995, **20**(2), 106–111.

65 **Grant, I.**, **Pan, X.**, **Wang, X.** and **Stewart, N.** Correction for viewing angle applied to PIV data obtained in aerodynamic blade vortex interaction studies. *Exps in Fluids*, 1994, **17**, 95–99.

66 **Bertuccioli, L.**, **Shridhar, G.** and **Katz, J.** Image shifting for PIV using birefringent and ferroelectric liquid crystals. In *Laser Anemometry*, FED Vol. 229, 1995, pp. 307–433 (American Society of Mechanical Engineers, New York).

67 **Landreth, C. C.** and **Adrian, R. J.** Electro optic image shifting for particle image velocimetry. *Appl. Optics*, 1988, **27**(20), 4216–4220 [reprinted in reference (**6**)].

68 **Lourenco, L. M.** Velocity bias technique for particle-image velocimetry measurements of high speed flows. *Appl. Optics*, 1993, **32**(12), 2159–2162.

69 **Hinsch, K.**, **Arnold, W.** and **Platten, W.** Turbulence measurements by particle imaging velocimetry. In *Optical Methods in Flow and Particle Diagnostics* (Ed. W. H. Stevenson), ICALEO '87, *LIA Proc.*, 1987, **63**, 127–134 [reprinted in reference (**6**)].

70 **Westerweel, J.**, **Dabiri, D.** and **Gharib, M.** Noise reduction by discrete image shifting in DPIV. In *Flow Visualisation*, Vol. VII (Ed. J. Crowder), 1995, pp. 688–699 (Begell Haue, New York).

71 **Swift, D. W.** Image rotation devices—a comparative study. *Optics and Laser Technol.*, 1972, **4**, 175–188.

72 **Kuboi, R.**, **Nienow, A. W.** and **Allsford, K.** A multi-purpose stirred tank facility for flow visualisation and dual impeller power measurement. *Chem. Engng Commun.*, 1983, **22**, 29–39.

73 **Wu, J., Pullum, L., Welsh, M. C.** and **Yunken, R.** Investigation of the relative flow field of an axial agitator impeller using a combined image shifting and de-rotation technique. In Proceedings of FED-Vol. 239 Fluids Engineering Division Conference, Vol. 4, 1996, pp. 655–660.

74 **Grant, I.** and **Liu, A.** Directional ambiguity resolution in particle image velocimetry by pulse tagging. *Exps in Fluids*, 1990, **10**, 71–76 [reprinted in reference (**6**)].

75 **Adamczyk, A. A.** and **Rimai, L.** 2-dimensional particle tracking velocimetry (PTV): technique and image processing algorithms. *Exps in Fluids*, 1988, **6**, 373–380 [reprinted in reference (**6**)].

76 **Farrugia, N.**, **Kanne, S.** and **Greenhalgh, D. A.** Three-pulse digital particle image velocimetry. *Optics Lett.*, 1995, **17**(20), 1827–1829.

77 **Coupland, J. M., Pickering, C. J. D.** and **Halliwell, N. J.** Particle image velocimetry: theory of directional ambiguity removal using holographic image separation. *Appl. Optics*, 1987, **26**, 1576–1578.

78 **Hussain, F.**, **Liu, D. D.**, **Simmons, S.** and **Meng, H.** Holographic particle velocimetry: prospects and limitations. In *Holographic Particle Image Velocimetry*, ASME FED Vol. 148 (Ed. P. Rood), 1993, pp. 1–11 (American Society of Mechanical Engineers, New York).

79 **Laurenco, L.** and **Wiffen, M. C.** Laser speckle methods in fluid dynamics applications. In *Laser Anemometry in Fluid Mechanics*, Vol. II (Ed. R. Adrian), 1986, pp. 51–68 (Ladoan-IST, Lisbon) [reprinted in reference (**6**)].

80 **Sinha, S. K.** Improving the accuracy and resolution of particle image or laser speckle velocimetry. *Exps in Fluids*, 1988, **6**, 67–68 [reprinted in reference (**6**)].

81 **Grant, I.** and **Liu, A.** Accuracy considerations in incoherent analysis of PIV images. *Appl. Optics*, 1989, **28**, 4508–4510.

82 **Perkins, R. J.** and **Hunt, J. C. R.** Particle tracking in turbulent flows. In *Advances in Turbulence*, Vol. 2, 1989, pp. 289–291 (Springer-Verlag, Berlin).

83 **Guezenec, Y.** and **Kiritis, N.** Statistical investigation of errors in particle image velocimetry. *Exps in Fluids*, 1990, **10**, 138–146 [reprinted in reference (**6**)].

84 **Grant, I.** and **Owens, E. H.** Confidence interval estimates in PIV measurements of turbulent flows. *Appl. Optics*, 1990, **29**(10), 1400–1402.

85 **Cenedese, A., Miozzi, M.** and **Romano, G. P.** Error detection in the analysis of PTV images using proper orthogonal decomposition. In Proceedings of Eighth International Symposium on *Application of Laser Techniques to Fluid Mechanics*, Lisbon, 1996, paper 27.3.

86 **Keane, R. D.**, **Adrian, R. J.** and **Zhang, Y.** Super-resolution particle image velocimetry. *Measmt Sci. Technol.*, 1995, **6**, 754–768.

87 **Hart, D. P.** Sparse array image correlation. In Proceedings of Eighth International Symposium on *Application of Laser Techniques to Fluid Mechanics*, Lisbon, 1996, paper 21.1.

88 **Willert, C. E.** and **Gharib, M.** Digital particle image velocimetry. *Exps in Fluids*, 1991, **10**, 181–193 [reprinted in reference (**6**)].

89 **Merzkirch, W.**, **Mrosewski, T.** and **Wintrich, H.** Digital particle image velocimetry applied to a natural convective flow. *Acta Mechanica*, 1994, **4** (Suppl. 1), 19–26.

90 **Lim, W. L.**, **Chew, Y. T.**, **Chew, T. C.** and **Low, H. T.** Improving the dynamic range of particle tracking velocimetry systems. *Exps in Fluids*, 1994, **17**, 282–284.

91 **Kimura, I.** and **Takamori, T.** Image processing of flow around a circular cylinder by using correlation technique. In *Flow Visualisation*, Vol. IV (Ed. C. Veret), 1986, pp. 221–226 (Hemisphere, Washington).

92 **Westerweel, J.** and **Nieuwstadt, S. T. M.** Performance tests on three-dimensional velocity measurements with a two camera DPIV. *Trans. ASME, Laser Anem.*, 1991, **1**, 349–355.

93 **Okada, E.**, **Enomoto, H.**, **Fukuoka, Y.** and **Minamitani, H.** Instantaneous imaging velocimeter with electronic specklegram. In Proceedings of Fifth International Symposium on *Applications of Laser Anemometry to Fluid Mechanics*, Lisbon, 1990, paper 18.2.

94 **Westerwell, J.** and **Niewestadt, F. T. M.** Measurements of the dynamics of coherent flow structures using particle image velocimetry. In Proceedings of Fifth International Symposium on *Applications of Laser Anemometry to Fluid Mechanics*, 1990, paper 18.3, pp. 476–499 (Springer-Verlag, Berlin, Heidelberg) [reprinted in reference (**6**)].

95 **Brystan-Cross, P. J., Judge, T. R., Quan, C., Pugh, G.** and **Corby, N.** The application of digital particle velocimetry (DPIV) to transonic flows. *Proc. Aerospace Sci.*, 1995, **31**, 1–17.

96 **Stasicki, B.** and **Meier, G. E. A.** A computer controlled, ultra high-speed video camera system. In Proceedings of Twenty-first International Congress on *High-speed Photography and Photonics*, Taejon, Korea, August 1994, SPIE Vol. 2513, 1994, pp. 196–208. Elektro. Hochgischwindigkeitskamera, Pat. 42 12271, 1992.

97 **Raffel, M.**, **Kompenhans, J.**, **Stasicki, B.**, **Bretthauer, B.** and **Meier, G. E. A.** Velocity measurement of compressible airflows utilizing a high speed video camera. *Exps in Fluids*, 1995, **18**, 204–215.

98 **Roth, G.**, **Hart, D.** and **Katz, J.** Feasibility of using the L64720 video motion estimation processor (MEP) to increase efficiency of velocity map generation of particle image velocimetry (PIV). In *Laser Anemometry*, FED-Vol. 229, 1995, pp. 387–393 (American Society of Mechanical Engineering, New York).

99 **Hernan, M. A.** and **Jiminez, J.** Computer analysis of a high-speed film of the plane turbulent mixing layer. *J. Fluid Mechanics*, 1982, **119**, 323–345.

100 **Vogel, A.** and **Lauterborn, W.** Time resolved particle image velocimetry used in the investigation of cavitation bubble dynamics. *Appl. Optics*, 1988, **27**(9), 1869–1876 [reprinted in reference (**6**)].

101 **Oakley, T.**, **Loth, E.** and **Adrian, R. J.** Cinematic particle image velocimetry of a turbulent free shear layer. In twenty-fifth AIAA Plasmadynamics and Lasers Conference, Colorado Springs, Colorado, 1994, paper AIAA 94-2298.

102 **Chang, T. P.**, **Wilcox, N. A.** and **Tatterson, G. B.** Application of image processing to the analysis of three-dimensional flow fields. *Opt. Engng*, 1984, **23**(3), 283–287 [reprinted in reference (**6**)].

103 **Thompson, B. J.** Holographic methods for particle size and velocity measurement—recent advances. In *Holographic Optics II: Principles and Applications (Proc. SPIE 1136)* (Ed. G. M. Morris), 1989, pp. 308–326 [reprinted in reference (**6**)].

104 **Utami, T.** and **Ueno, T.** Visualization and picture processing of turbulent flow. *Exps in Fluids*, 1984, **2**, 25–32 [reprinted in reference (**6**)].

105 **Grant, I.**, **Zhao, Y.**, **Tan, Y.** and **Stewart, J. N.** Three component flow mapping; experiences in stereoscopic PIV and holographic velocimetry. In Proceedings of Fourth International Conference on *Laser Anemometry, Advances and Applications*, 1991, pp. 365–371 (American Society of Mechanical Engineers, New York) [reprinted in reference (**6**)].

106 **Wolf, P. R.** *Elements of Photogrammetry*, 1974 (McGraw-Hill, London, New York).

107 **Spedding, G. R.**, **Rayner, J. M.** and **Pennycuick, C. J.** Momentum and energy in the wake of a pigeon (*Columa livia*) in slow flight. *J. Expl Biol*., 1984, **11**, 81–102.

108 **Grant, I.**, **Fu, S.**, **Pan, X.** and **Wang, X.** The application of an in-line, stereoscopic, PIV system to 3-component velocity measurements. *Exps in Fluids*, 1995, **19**, 214–221.

109 **Guezennec, Y. G.**, **Zhao, Y.** and **Gieseke, T. J.** High-speed 3D scanning particle image velocimetry (3D SPIV) technique. Proceedings of Seventh International Symposium on *Applications of Laser Techniques to Fluid Mechanics*, Lisbon, 1994, paper 26.1.

110 **Hinsch, K. D.** Three-dimensional particle image velocimetry. *Measmt Sci. Technol*., 1995, **6**, 742–753.

111 **Palero, V.** and **Arroyo, P.** Size and velocity measurements in a two phase flow using stereoscopic particle image velocimetry. In Proceedings of Eighth International Symposium on *Application of Laser Techniques to Fluid Mechanics*, Lisbon, 1996, paper 12.3.

112 **Dracos, T.** and **Malik, N. A.** 3D particle tracking velocimetry—its possibilities and limitations. In *Flow Visualisation*, Vol. VI (Eds Y. Tanida and H. Miyashiro), 1992, pp. 785–791 (Springer-Verlag, Berlin).

113 **Weinstein, L. M.**, **Beeler, G. B.** and **Lindermann, A. M.** High-speed holocinematographic velocimeter for studying turbulent flow control physics. AIAA paper 85-0526, 1985, pp. 1–9.

114 **Meng, H.** and **Hussain, F.** Holographic particle velocimetry: a 3D measurement technique for vortex interactions, coherent structures, and turbulence. *Fluid Dyn. Res*., 1991, **8**, 33–52.

115 **Haussmann, G.** and **Lauterborn, W.** Determination of size and position of fast moving gas bubbles in liquids by digital 3-D image processing of hologram reconstructions. *Appl. Optics*, 1980, **19**(20), 3529–3535.

116 **Blackshire, J. L.**, **Humphreys, W. M.** and **Bartram, S. M.** 3-dimensional, 3-component velocity measurements using holographic particle image velocimetry (HPIV). In Eighteenth AIAA Aerospace Ground Testing Conference, Colorado Springs, 1994, paper 94-2645.

117 **Barnhart, D. H.**, **Adrian, R. J.** and **Papen, G. C.** Phase-conjugate holographic system for high-resolution particle image velocimetry. *Appl. Optics*, 1994, **33**(30), 7159–7170.

118 **Coupland, J. M.** and **Halliwell, N. A.** Particle image velocimetry: three dimensional fluid velocity measurements using holographic recording and optical correlation. *Appl. Optics*, 1992, **31**, 1005–1007 [reprinted in reference (**6**)].

119 **Zhang, J.** and **Katz, J.** Three dimensional velocity measurements using hybrid HPIV. In Proceedings of Eighth International Symposium on *Application of Laser Techniques to Fluid Mechanics*, Lisbon, 1996, paper 4.3.

120 **Parker, S. C. J.**, **Holden, C. M. E.** and **Brystan-Cross, P. J.** Study of transonic flows by quantitative holographic interferometry. *Proc. Instn Mech. Engrs., Part G*, 1994, **208** (G2), 91–97.

121 **Karurandani, T.**, **Funakoshi, M.** and **Oikawa, M.** Breakdown and rearrangement of vortex streets in a far wake. *J. Phys. Soc. Japan*, 1989, **58**(5), 1597.

122 **Cenedese, A.** and **Paglialunga, A.** New technique for the determination of the third velocity component with PIV. *Exps in Fluids*, 1988, **8**, 228–230 [reprinted in reference (**6**)].

123 **Dinkelacker, F.**, **Schafer, M.**, **Ketterle, W.** and **Wolfrum, J.** Determination of the third velocity component with PTA using an intensity graded light sheet. *Exps in Fluids*, 1992, **13**, 357–359.

124 **Stolz, W.** and **Kohler, J.** In-plane determination of 3D-velocity vectors using particle tracking anemometry (PTA). *Exps in Fluids*, 1994, **17**, 105–109.

125 **Willert, C. E.** and **Gharib, M.** Three dimensional particle imaging with a single camera. *Exps in Fluids*, 1992, **12**, 353–358 [reprinted in reference (**6**)].

126 **Robinson, O.** and **Rockwell, D.** Construction of three-dimensional images of flow structure via particle tracking techniques. *Exps in Fluids*, 1993, **14**, 257–270.

127 **Timmerman, B. H.** and **Watt, D. W.** Tomographic holographic interferometry for unsteady compressible flows. In Proceedings of International Symposium on *Optical Science*, *Engineering*, *and Instrumentation*, SPIE Bellingham, 1995, paper number 2546-40, pp. 287–296.

128 **Raffel, M.**, **Gharib, M.**, **Ronnenberger, O.** and **Kompenhans, J.** Feasibility study of three-dimensional PIV by correlating images of particles within parallel light sheet planes. *Exps in Fluids*, 1995, **19**, 69–77.

129 **Zhang, Y. W.** Optical measurement of velocity and acceleration with colour coding. *Opt. Laser Technol*., 1986, **18**, 256–258.

130 **Stefanini, J.**, **Cognet, G.**, **Vila, J. C.**, **Merite, B.** and **Brenier, Y.** A coloured method for PIV technique. In *Flow Visualisation and Image Analysis* (Ed. F. T. M. Nieuwstadt), 1993, pp. 247–258 (Kluwer Academic Publishers, The Netherlands).

131 **Cenedese, A.** and **Romano, G. P.** Comparison between classical and three-colour PIV in a wake flow. *J. Flow Visualisation and Image Processing*, 1993, **1**, 371–384.

132 **Towers, D. P.** and **Buckberry, C. H.** Application of two-colour PIV to in-cylinder flow velocity measurement. In IMechE Conference, 1996, paper C516/058/96.

133 **Goggineni, S. P.**, **Pestian, D. J.**, **Rivir, R. B.** and **Goss, L. P.** PIV measurements of flat plate film cooling flows with high free stream turbulence. In Thirty-fourth Aerospace Sciences Meeting and Exhibition, Reno, Nevada, January 1996, paper AIAA 96-0617.

134 **Gogineni, S.**, **Trump, D.**, **Rivir, R.**, **Goss, L.** and **Pestian, D.** High-resolution digital two-colour PIV (D2CPIV) and its application to high-free stream turbulent flows. In Proceedings of Eighth International Symposium on *Application of Laser Techniques to Fluid Mechanics*, Lisbon, 1996.

135 **Gogineni, S.**, **Rivir, R.**, **Pestian, D.** and **Goss, L.** High free-stream turbulence on turbine film cooling flows. *Phys. Fluids*, 1996, **8**(9), S4.

136 **Kawahashi, M.** and **Hosoi, K.** Beam-sweep laser speckle

velocimetry. *Exps in Fluids*, 1989, **8**, 109–111 [reprinted in reference (**6**)].

137 **Kawahashi, M.** and **Hosoi, K.** Dual-beam-sweep laser speckle velocimeter. *Exps in Fluids*, 1991, **11**, 278–280.

138 **Gray, C.**, **Greated, C. A.**, **McCluskey, D. R.** and **Easson, W. J.** An analysis of the scanning beam PIV illumination system. *Measmt Sci. Technol.*, 1991, **2**, 461–468.

139 **Castellini, P.** Calibration of a technique for direction ambiguity resolution in particle image velocimetry. In Proceedings Conference on *Electtroottica 94*, 3 Convegno Nazionale on *Strumentazione e Metodi di Misura Elettroottici*, Pavia, 25–27 May 1994.

140 **Cui, M. M.** and **Adrian, R. J.** Scanned two-colour particle image velocimetry. In *Flow Visualisation and Image Processing of Multiphase Systems*, FED Vol. 209, 1995, pp. 83–90 (American Society of Mechanical Engineers, New York).

141 **Dong, S.** A PIV study of the 3D flow behind a circular cylinder. PhD thesis, Fluid Loading and Instrumentation Centre, Heriot-Watt University, Edinburgh, 1990.

142 **Zhao, Y.**, **Gieseke, T. J.** and **Guezennec, Y. G.** 3D particle image velocimetry—a new technique. In Proceedings of Second International Conference on *Fluid Dynamic Measurement and Its Applications* (Eds X. Shen and X. Sun), Beijing, Tsinghua University, Beijing, PRC, pp. 286–291.

143 **Brucker, C.** Study of vortex breakdown by particle tracking velocimetry (PTV). Part 1: bubble-type vortex breakdown. *Exps in Fluids*, 1992, **13**, 339–349.

144 **Brucker, C.** and **Althaus, W.** Study of vortex breakdown by particle tracking velocimetry (PTV). Part 2: spiral type breakdown. *Exps in Fluids*, 1993, **14**, 133–139.

145 **Brucker, C.** Spatial correlation analysis for 3-D Scanning PIV: simulation and application of dual-colour light sheet scanning. In Proceedings of Eighth International Symposium on *Application of Laser Techniques to Fluid Mechanics*, Lisbon, 1996, paper 4.2.

146 **Anderson, D. J.**, **Morgan, R. D.**, **McCluskey, D. R.**, **Jones, J. D. C.**, **Easson, W. J.** and **Greated, C. A.** An optical fibre delivery system for pulsed laser particle image velocimetry illumination. *Measmt Sci. Technol.*, 1995, **6**, 809–814.

147 **Grant, I.** and **Wang, X.** Directionally-unambiguous, digital particle image velocimetry studies using an image intensifier camera. *Exps in Fluids*, 1995, **18**, 358–362.

148 **Grant, I., Owens, E. H.** and **Smith, G. H.** Parallel (DAP) and serial computer methods for image processing in pulsed laser velocimetry. In Proceedings of Fourth International Symposium on *Optical and Optoelectronic Applied Science and Engineering*, Hague, The Netherlands, 1987.

149 **Meinhart, C. D.**, **Prasad, A. K.** and **Adrian, R. J.** Parallel digital processor system for particle image velocimetry. *Measmt Sci. Technol.*, 1993, **4**, 619–626.

150 **Sridhar, G.** and **Katz, J.** Drag and lift forces on microscopic bubbles entrained by a vortex. *Phys. Fluids*, 1995, **7**(2), 389–399.

151 **Chu, S.**, **Dong, R.** and **Katz, J.** Relationship between unsteady flow, pressure fluctuations, and noise in a centrifugal pump—Part A: use of PDV data to compute the pressure field. *Trans. ASME*, 1995, **117**, 24–29.

152 **Grant I.**, **Smith, G. H.**, **Infield, D. G.**, **Zhao, Y.**, **Fu, S.**, **Owens, E.** and **Reinbold, P.** Laboratory and field experiences in the application of particle image velocimetry to wind turbines. In Proceedings of Conference on *Optical Diagnostics in Fluid and Thermal Flow*, SPIE Technical Conference 2005, San Diego, July 1993, paper 2005–46, pp. 467–477.

153 **Aroussi, A., Yan, Y.-Y.** and **Grant, I.** Experimental verification of numerical simulation of turbulent flow past enclosures in offshore structures. *Optics and Lasers in Engng*, 1992, **16**, 391–409.

154 **Grant, I., Owens, E., Stewart, J. N.** and **Aroussi, A.** Particle image velocimetry measurements of propeller–hull wake interaction behind a model ship. In Proceedings of Sixth International Symposium on *Applications of Laser Techniques to Fluid Mechanics*, Lisbon, 20–23 July, 1992, paper 39.3.

155 **Oschwald, M.**, **Guerra, R.** and **Waidmann, W.** Investigation of the flowfield of a scramjet combustor with parallel H_2 injection through a strut by particle image displacement velocimetry. In Third International Symposium on *Special Topics in Chemical Propulsion*, Scheveningen, The Netherlands, 10–14 May 1993, pp. 498–504.

156 **Horner, M.**, **Stewart, J. N.**, **Galbraith, R. A. McD.**, **Grant, I.**, **Coton, F. N.** and **Smith, G. H.** An examination of vortex deformation during blade–vortex interaction utilising particle image velocimetry. *Am. Inst. Aeronaut. Astronaut. J.*, 1996, **34**(6), 1188–1194.

157 **Wiegel, M.** and **Fischer, M.** Proper orthogonal decomposition applied to PIV data for the oblique transition in a Blasius boundary layer. In SPIE Proceedings of International Symposium on *Optical Science, Engineering and Instrumentation*, San Diego, 1995, paper 2546-14.

158 **Corino, E. R.** and **Brodkey, R. S.** A visual investigation of the wall region in turbulent flow. *J. Fluid Mechanics*, 1969, **37**(1), 1–30.

159 **Draad, A. A.** and **Westerweel, J.** Measurement of temporal and spatial evolution of transitional pipe flow with PIV. In Proceedings of Eighth International Symposium on *Application of Laser Techniques to Fluid Mechanics*, Lisbon, 1996, paper 29.3.

160 **Meinhart, C. D.** and **Adrian, R. J.** Measurement of the zero-pressure gradient turbulent boundary layer using particle image velocimetry. In Thirty-third Aerospace Sciences Meeting and Exhibit, Reno, Nevada, 1995, paper AIAA 95-0789.

161 **Reuss, D. L.**, **Adrian, R. J.** and **Landreth, C. C.** Two dimensional velocity measurements in a laminar flame using particle image velocimetry. *Combust. Sci. and Technol.*, 1989, **67**, 73–83.

162 **Mungal, M. G.**, **Lourenco, L. M.** and **Krothapalli, A.** Instantaneous velocity measurements in laminar and turbulent premixed flames using on-line PIV. *Combust. Sci. and Technol.*, 1995, **106**, 239–265.

163 **Muniz, L., Martinex** and **Mungal, M. G.** Application of PIV to turbulent reacting flows. In Proceedings of Eighth International Symposium on *Application of Laser Techniques to Fluid Mechanics*, Lisbon, 1996, paper 3.3.

164 **Paone, N., Revel, G. M.** and **Nino, E.** Velocity measurement in high turbulent premixed flames by a PIV measurement system. In Proceedings of Eighth International Symposium on *Application of Laser Techniques to Fluid Mechanics*, Lisbon, 1996, paper 3.4.

165 **Brandt, A.** and **Merzirch, W.** Particle image velocimetry applied to a spray jet. *Particle System Charact*., 1994, **2**, 156–158.

166 **Fick, W., Griffiths, A. J.** and **O'Doherty, T.** Visualisation of coherent structures in a highly turbulent swirling flame. In Proceedings of Eighth International Symposium on *Application of Laser Techniques to Fluid Mechanics*, Lisbon, 1996, paper 10.4.

167 **Tashtoush, G., Narumi, A., Ito, A., Saito, K.** and **Cremers, C.** Combined techniques of holographic interferometer and particle track laser sheet to study flame spread over liquids. In Proceedings of Eighth International Symposium on *Application of Laser Techniques to Fluid Mechanics*, Lisbon, 1996, paper 11.3.

168 **Khabakhpasheva, E. M., Orlov, V. V., Yefimenko, G. I.** and **Karsten, V. M.** Simultaneous registration of three components of instantaneous velocity vectors in the near-wall turbulent flow. *Thermophysics and Aeromechanics*, 1994, **1**(2), 165–170.

169 **Hilgers, S., Merzkirch, W.** and **Wagner, T.** PIV measurements in multiphase flow using CCD- and photo camera. In *Flow Visualisation and Image Processing of Multiphase Systems*, FED-Vol. 209, 1995, pp. 151–154 (American Society of Mechanical Engineers, New York).

170 **Anderson, S. L.** and **Longmire, E.** Particle motion in the stagnation zone of an impinging air jet. *J. Fluid Mechanics*, 1995, **229**, 333–366.

171 **Faure, M., Heikal, M. R.** and **Jackson, N.** PIV measurements and characterisation of in-cylinder flows in combustion engines. In Proceedings of Eighth International Symposium on *Application of Laser Techniques to Fluid Mechanics*, Lisbon, 1996, paper 22.3.

172 **Reeves, M., Garner, C. P., Dent, J. C.** and **Halliwell, N. A.** Study of barrel swirl in a four-valve optical IC engine using particle image velocimetry. In Proceedings of Third International Symposium on *Diagnostics and Modelling of Combustion in Internal Combustion Engines*, Yokohama, Japan, 1994, pp. 429–435.

173 **Zhou, M.** and **Garner, C. P.** Particle image velocimetry measurements of the flow field within an enclosed rotating disc–stator system and comparisons with computational fluid dynamics results. *Opt. Diagnostics in Engng* (*ODE*) *Electronic Hyperjournal*, 1996, **1**(2), 9–21 (http://www.civ.hw.ac.uk/research/flic/ode/odemain.htm).

174 **Casey, M. V., Eisele, K., Zhang, Z., Gutlich, J.** and **Schachenmann, A.** Flow analysis in a pump diffuser, Part 1: LDA and PTV measurements of the unsteady flow. ASME Summer Meeting, Symposium on *Laser Anemometry*, 1995, 89–100.

175 **Graham, L. J. W.** and **Soria, J.** Near wake of an inclined cylinder. Proceedings of International Colloquium on *Jets, Wakes and Shear Layers*, Melbourne, Australia, 1994, paper 7, pp. 1–8.

176 **Wu, J., Sheridan, J., Welsh, M. C.** and **Hourigan, K.** Three dimensional vortex structures in a cylinder wake. *J. Fluid Mechanics*, 1996, **312**, 201–222.

177 **Corlett, A. E.** and **Barnes, F. H.** On a discontinuity in the laminar regime of the flow around a circular cylinder. *Europhys. Lett*., 1996, **34**(3), 180–193.

178 **Hirt, F., Jud, E.** and **Zhang, Z.** Investigation of the local flow topology in the vicinity of a prosthetic heart valve using particle image velocimetry. In Proceedings of Seventh International Symposium on *Applications of Laser Techniques to Fluid Mechanics*, Lisbon, 1994, paper 37.3.

179 **Lim, W. L., Chew, Y. T., Chew, T. C.** and **Low, H. T.** Particle image velocimetry in the investigation of flow past artificial heart valves. *Annuals of Biomed. Engng*, 1994, **22**, 307–308.

180 **Lattimer, S. B., Braun, M. J.** and **Dzodzo, M.** Simultaneous visualisation of flow and temperature patterns in a shell and tube heat exchanger by TLC. In *Experimental and Numerical Flow Visualisation*, FED-Vol. 218, 1995, pp. 7–14 (American Society of Mechanical Engineers, New York).

181 **Grant, I.** and **Smith, G. H.** Modern developments in particle image velocimetry. *J. Optics and Lasers in Engng*, 1988, **9**, 245–264 [reprinted in reference (**6**)].

182 **Skyner, D. J., Gray, C.** and **Greated, C. A.** A comparison of time-stepping numerical predictions with whole-field flow measurement in breaking waves. In *Water Wave Kinematics* (Eds Torum and Gudmestad), 1990, pp. 491–508 (Kluwer Academic Publishers, The Netherlands).

183 **Liu, A., Shen, X., Smith, G. H.** and **Grant, I.** Particle image velocimetry measurements of wave–current interaction in a laboratory flume. *Optics and Lasers in Engng*, 1992, **16**, 239–264.

184 **Shankar, N. J., Cheong, H. F., Nallayarasu, S.** and **Idicahndy, V. G.** Investigation of particle kinematics around a submerged horizontal plate by particle image velocimetry. In Proceedings of Ninth Congress of Asian and Pacific Division of the International Association for Hydraulic Research, Singapore, 1994, pp. 58–66.

185 **Gottero, M.** and **Onorato, M.** Two-scale grid and turbulence mixing. In Proceedings of Eighth International Symposium on *Application of Laser Techniques to Fluid Mechanics*, Lisbon, 1996, paper 35.1.

186 **Grant, I.** FLIC WWW site PIV animation (http://www.civ.hw.ac.uk/research/flic/pivig.htm).

187 **Carvalho, I. S.** and **Heitor, M. V.** Visualisation of vortex breakdown in turbulent unconfined jet flow. *Opt. Diagnostics in Engng* (*ODE*) *Electronic Hyperjournal*, 1996, **1**(2), 22–30 (http://www.civ.hw.ac.uk/research/flic/ode/odemain.htm).

188 **Collicott, S. H.** Transition from particle image velocimetry to laser speckle velocimetry with increasing density. In *Applications of Laser Techniques to Fluid Mechanics* (Ed. R. J. Adrian), 1993, pp. 181–194 (Springer-Verlag, Berlin).